



Obrabotka metallov -

Metal Working and Material Science











Journal homepage: http://journals.nstu.ru/obrabotka_metallov



Research and analysis of electrical discharge machining in the manufacture of products from heat-resistant alloys: a literature review

Evgeniy Shlykov^{a,*}, Timur Ablyaz^b, Vladimir Blokhin^c, Karim Muratov^d, Ilya Osinnikov^e

Perm National Research Polytechnic University, 29 Komsomolsky prospekt, Perm, 614990, Russian Federation

^a  <https://orcid.org/0000-0001-8076-0509>,  Kruspert@mail.ru; ^b  <http://orcid.org/0000-0001-6607-4692>,  lowrider11-13-11@mail.ru;
^c  <https://orcid.org/0009-0009-2693-6580>,  warkk98@mail.ru; ^d  <http://orcid.org/0000-0001-7612-8025>,  Karimur_80@mail.ru;
^e  <https://orcid.org/0009-0006-4478-3803>,  ilyuhaosinnikov@bk.ru

ARTICLE INFO

Article history:

Received: 11 June 2025

Revised: 04 July 2025

Accepted: 09 September 2025

Available online: 15 December 2025

Keywords:

Electrical discharge machining

Heat-resistant alloys

Experimental studies

Working fluid

Surface roughness

Accuracy

Microcracks

Surface layer

ABSTRACT

Introduction. In modern mechanical engineering, there is a growing trend toward the development and implementation of novel heat-resistant alloys with enhanced physical and mechanical properties. Electrical discharge machining (*EDM*) is a promising method for manufacturing products from these new-generation heat-resistant alloys. This paper presents an analysis of current research in the field of *EDM* of heat-resistant alloys. The primary focus is on analyzing output qualitative and quantitative indicators in relation to input parameters – machining mode and conditions. The key factors influencing the efficiency of *EDM* are considered, including machining parameters and the composition of the working fluid and electrode material. This analysis of current research is intended for specialists in the field of heat-resistant alloy machining, developers of *EDM* technologies, and researchers working to improve manufacturing methods for aircraft engine components. **The purpose of this work** is to conduct a literature review of existing research on modern methods for ensuring and improving the efficiency and quality of electrical discharge machining (*EDM*) of heat-resistant materials. **The methods of investigation** involved a theoretical analysis of current research on electrical discharge machining of heat-resistant alloys. **Results and discussion.** A literature analysis was conducted, and it revealed that current strength and pulse duration are the main technological parameters determining the quality of the processed surface and the material removal rate. The effectiveness of using modified working fluids (with graphene and carbon nanotubes) during heat-resistant material processing to improve surface quality was confirmed. It is of particular interest to conduct experimental studies on the influence of adding various material components to the working fluid to improve surface quality indicators after complex pulse electrical discharge machining (*CPEDM*) and to assess the impact of these alloying materials on the surface layer of heat-resistant materials.

For citation: Shlykov E.S., Ablyaz T.R., Blokhin V.B., Muratov K.R., Osinnikov I.V. Research and analysis of electrical discharge machining in the manufacture of products from heat-resistant alloys: a literature review. *Obrabotka metallov (tekhnologiya, oborudovanie, instrumenty)* = *Metal Working and Material Science*, 2025, vol. 27, no. 4, pp. 16–47. DOI: 10.17212/1994-6309-2025-27.4-16-47. (In Russian).

Introduction

The key driver of modern industry is the active development and implementation of novel heat-resistant materials possessing a specific set of mechanical and physical-chemical properties. These characteristics ensure the retention of strength properties in structural components of equipment and machinery throughout their service life. Numerous research teams are dedicated to investigating the effects of various processing methods on the characteristics of heat-resistant alloys, which are critical for key industries such as aerospace engine manufacturing, power generation (including nuclear power), and the automotive industry. High resistance to corrosion and oxidation, enhanced ductility, heat resistance, mechanical strength, and excellent fatigue and creep resistance even at elevated temperatures – these properties make heat-resistant

* Corresponding author

Shlykov Evgeniy S., Ph.D. (Engineering), Associate Professor
Perm National Research Polytechnic University,
29 Komsomolsky prospekt,
614990, Perm, Russian Federation
Tel.: +7 961 759-88-49, e-mail: Kruspert@mail.ru

alloys superior to other classes of materials. Most heat-resistant alloys are primarily nickel-based. Due to their excellent high-temperature mechanical and chemical properties — including high heat resistance, thermal shock resistance, enhanced fatigue strength, high fracture toughness, phase stability, superior erosion and corrosion resistance, improved ductility and toughness, and high melting point — nickel-based alloys can operate for extended periods in aggressive service environments. Active research into heat-resistant materials stems from their strategic importance for critical technological development, the continuous demand for improved material characteristics, and the expansion of their application areas in modern industry. International research primarily focuses on the nickel-based superalloy *Inconel* [1–7] and its various grades, which differ in the type and concentration of alloying elements. The properties of heat-resistant materials are tailored by specific alloying elements:

- **Nickel**, as the primary base, contributes to the alloy's ductility, toughness, and heat capacity.
- **Molybdenum** and **tungsten** enhance creep resistance and high-temperature mechanical strength.
- **Vanadium**, typically in small quantities, improves overall high-temperature properties.
- **Niobium** prevents intergranular corrosion.
- **Titanium** enhances corrosion resistance.
- **Cobalt** increases relaxation resistance.

As reported in studies [8–15], nickel-based alloys are widely used in many critical components of aerospace engines and gas turbines, particularly in parts exposed to high temperatures, such as jet turbine blades, turbocharger vanes, and combustion chambers. Nickel-based alloys can account for approximately half of the total mass of aircraft engines. Beyond the aerospace sector, nickel-based alloys are also employed in nuclear reactors, food processing, shipbuilding, environmental protection facilities, and petrochemical industries, among others. Current research on heat-resistant alloys emphasizes compositions containing refractory transition metals (molybdenum, tungsten, tantalum, rhenium, and ruthenium). Promising domestic heat-resistant alloys include

- *VV751P* (Cr-56 %Ni-Co-V-Mn-Ti-Al-B);
- *ZhS6* (Cr-57% Ni-V-Co-Al-Ti-Mn-B),
- *KhN70Yu* (Cr-70% Ni-Al)
- *KhN60VT* (Cr-60% Ni-V-Ti),
- *KhN65VMTYu* (Cr-65% Ni-V-Mn-Ti-Al),
- *KhN55VMTKYu* (Cr-55% Ni-V-Mn-Ti-Co-Al),
- *KhN78T* (Cr-78% Ni-Ti),
- *EP741NP* (XH51KBMTIOB Cr-51% Ni-Co-B-Mn-Ti-Al-B),
- *EI698* (Cr-73% Ni-Mn-B-Ti-Al) [16–18].

The machining of heat-resistant alloys is complicated by several inherent properties, including low thermal conductivity, high melting points, significant work hardening effects, susceptibility to burr formation, the generation of high cutting forces, chemical affinity with tool materials, and the presence of abrasive carbide particles in their microstructure. These properties are exacerbated by elevated temperatures during machining, which significantly increase the load on the cutting edge, intensify tool wear, and necessitate wear compensation in the machine's control program. Furthermore, plastic deformation of these materials is challenging due to their austenitic face-centered cubic (FCC) crystal structure, which exhibits low yield strength despite possessing high ultimate tensile strength. Their inherent abrasiveness, often intensified by the presence of hard carbide inclusions and other abrasive particles, leads to severe tool wear and significantly reduced tool life. Heat-resistant alloys are classified as difficult-to-machine materials. The combination of these issues severely limits the achievable precision and overall efficiency in the machining of such alloys [19–24].

Electrical discharge machining (EDM) has emerged as a promising method for processing heat-resistant materials, drawing significant interest from scientific communities. This paper presents a review of scientific literature focused on the electrical discharge machining (EDM) process of heat-resistant alloys.

The purpose of this work is to conduct a literature review of existing research on modern methods for ensuring and improving the efficiency and quality of electrical discharge machining (*EDM*) of heat-resistant materials.

To achieve this purpose, the following research **tasks** were undertaken:

- Classification of key *EDM* process parameters and modern methods for their optimization;
- Determination of the advantages, disadvantages, and limitations of these modern methods for enhancing the efficiency and quality of electrical discharge machining of heat-resistant materials;
- Identification of current development trends for these methods.

Research methodology

A comprehensive literature review has been conducted on research in the field of electrical discharge machining (*EDM*) of heat-resistant materials, focusing on methods for ensuring surface integrity and improving *EDM* efficiency. Various methods for increasing *EDM* efficiency and enhancing surface integrity are described, along with their limitations, advantages, and disadvantages. The main trends in the development of modern methods for ensuring and improving *EDM* efficiency during the machining of heat-resistant alloys are identified.

Results and Discussion

The main advantages of *EDM* are presented in Fig. 1.

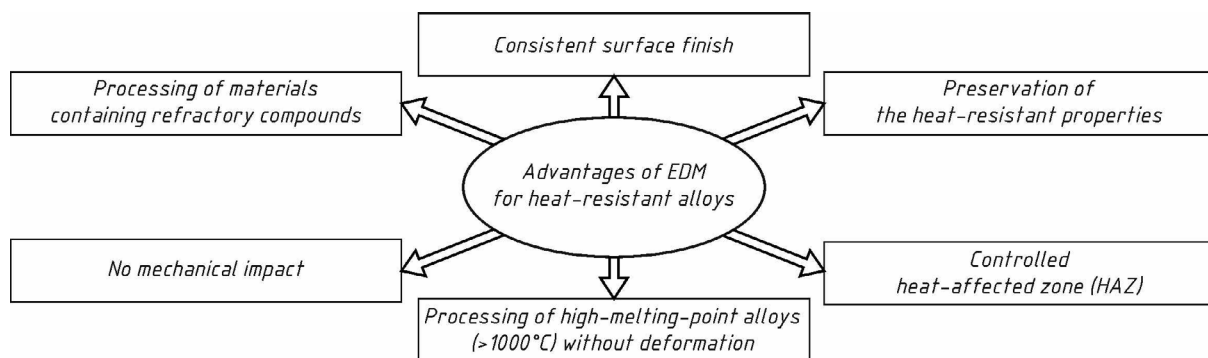


Fig. 1. Advantages of the *EDM* process

Table presents an analysis of research trends focusing on the output parameters of wire electrical discharge machining (*WEDM*) and copy-piercing electrical discharge machining (*EDM*) of heat-resistant alloys. *EDM* of heat-resistant materials often results in crack formation on the machined surfaces and the transfer of particles from the tool electrode and working fluid to the surface, thereby altering the characteristics of the surface layer. This redeposition of tool electrode particles and working fluid degradation products compromises the operational properties of the machined products. This is attributed to the non-uniform surface microstructure (including microcracks and other surface defects) and the softening of the surface layer.

Consequently, a critical review of modern solutions for ensuring surface integrity and preserving operational properties during electrical discharge machining of heat-resistant alloys is a crucial undertaking.

The main research trends concerning the *EDM* process of heat-resistant alloys are presented in Fig. 2.

A literature review on modern *EDM* studies revealed that authors' attention is primarily focused on investigating the influence of parameters such as current in the interelectrode gap (*IEG*), the duration of the electrical pulses (t_{on}), voltage (U), polarity, tool electrode material, tool electrode geometry, the size of the machined surface, as well as the working fluid characteristics (e.g., type, purity, feed rate, filtration system). These parameters are studied for their impact on processing quality indicators, specifically surface roughness and the modified surface layer (recast layer).

Directions of scientific papers studying the *WEDM* and *EDM* processes of heat-resistant alloys

No.	Variation parameters	Output parameters	Paper number
1	T_{on} , T_{off} , h , Working fluid	Surface roughness	25–41
2	T_{on} , I , P	Wear coefficient	32, 42–47
3	T_{on} , T_{off} , h	Cutting width for <i>WEDM</i>	48–51
4	T_{on} , T_{off} , I , U Polarity	Size of defective (white) layer	32, 39–40, 54–60
5	<i>ET</i> Material, I , T_{on}	Quality indicators (presence of cracks)	39, 43–45, 57, 69
6	Flushing of <i>IEG</i>	Surface roughness, precision of <i>EDM</i> processing, productivity	75–77

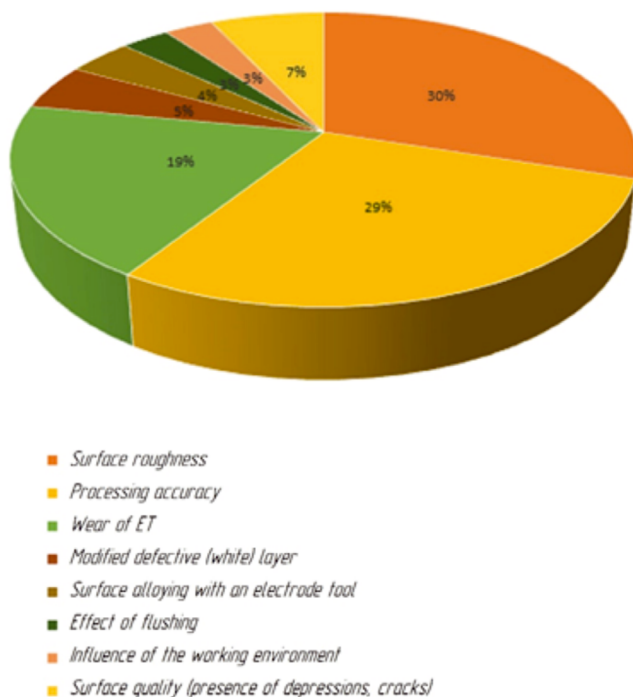


Fig. 2. Main trends in scientific research of the *EDM* process of heat-resistant alloys

Surface quality indicator after *EDM*: roughness (Ra)

The studies of the *WEDM* process in [25–31] investigated the processing of *Inconel 625* using an orthogonal experimental design, where various processing parameters were selected: current (I), pulse-on time (t_{on}), and pulse-off time (t_{off}). Response models were developed, and the authors found that the greatest influence on surface quality, specifically Ra roughness, is exerted by parameters such as pulse-on time (t_{on}) and current (I). In [25, 29], it was noted that a low discharge current contributes to the formation of a smoother machined surface, which is attributed to a more accurately controlled process of single discharge formation. Furthermore, adjusting the pulse-on time with a correctly selected mode promotes uniform melting of the material on the workpiece surface, evaporation, and removal from the processing zone, which has a favorable effect on surface finish. In all studies, the best roughness values were obtained with a pulse-on time of 100 to 110 μs , while the current was 7–9 A.

In [32], it was noted that to ensure the required surface roughness with minimal tool electrode wear in the *EDM* process, it is necessary to use minimal peak current and the shortest pulse duration. The authors found that the pulse duration had an insignificant effect on the surface roughness.

In [33–37], the authors investigated the influence of the input parameters of the *EDM* process on process productivity and surface roughness (Ra). Factorial experiments were conducted, and response functions were obtained, which showed that the pulse current had a greater influence on these parameters. With an increase in the current, process productivity increased, while the surface quality deteriorated compared to lower current settings.

In [38], experiments were conducted using the *Taguchi-Gray* analysis method for the *WEDM* of *Inconel 825*. The experiments showed that the pulse-on time and spark gap voltage had the greatest effect on surface roughness. It was found that the optimal parameters for *Inconel* processing were: pulse-on time of 105 μs , pulse-off time of 40 μs , and spark gap voltage of 30 V.

In [39], the authors investigated the effect of inclusions in the working fluid on surface roughness (Ra). The inclusions used were graphene and multi-walled carbon nanotubes. The studies were carried out in a

single processing mode at a pulse-on time of 35 μs , a current of 12 A, and a voltage of 40 V. The paper shows that with the addition of nanocarbon particles to the dielectric fluid, a smoother surface finish was achieved ($Ra = 4.836 \mu\text{m}$ with the addition of graphene and $Ra = 4.96 \mu\text{m}$ with the addition of carbon nanotubes) compared to conventional dielectric fluid ($Ra = 6.2 \mu\text{m}$). A comparative analysis of the results allows us to conclude that it is necessary to use a modified working fluid to improve the surface quality.

In [40], the authors conducted a study of the influence of the working fluid on the quality and topography of the surface (Fig. 3).

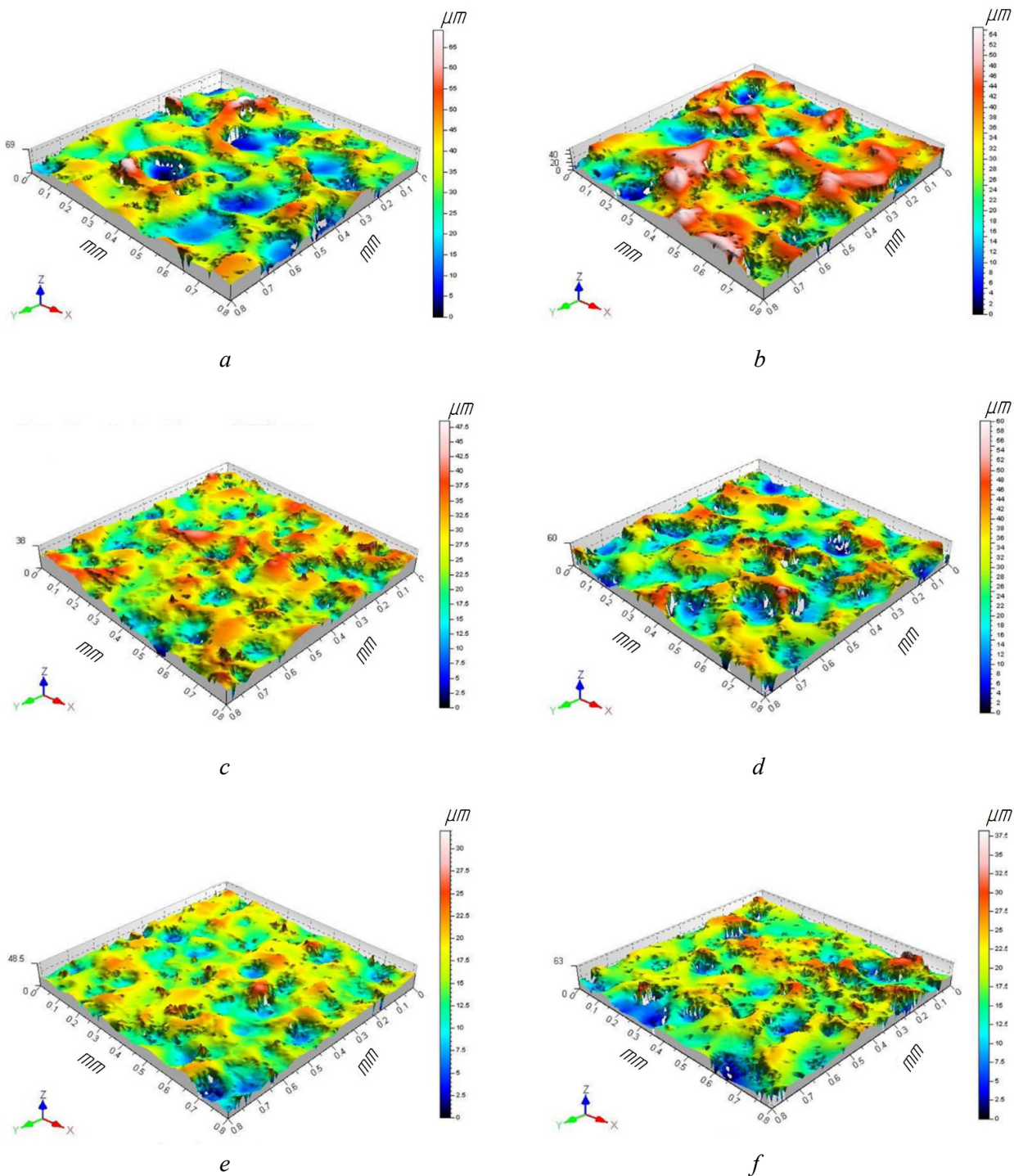


Fig. 3. Surface topography after EDM of AISi 1045 steel using deionized water as a dielectric (a, c, e):

a) at a current of 9 A and a pulse on-time of 100 μs , c) at a current of 3 A and a pulse on-time of 100 μs , e) at a current of 6 A and a pulse on-time of 100 μs ; and using kerosene as a dielectric (b, d, f): b) at a current of 6 A and a pulse on-time of 100 μs , d) at a current of 9 A and a pulse on-time of 100 μs ; f) at a current of 3 A and a pulse on-time of 100 μs [40]

The authors noted that current has the greatest impact on the formation of the surface characteristics and the incidence of surface defects. A direct correlation was observed: an increase in current resulted in a deterioration of all surface quality indicators. To achieve a smoother surface finish, minimum values of current and pulse duration should be employed.

In [41], the effect of processing parameters on surface roughness (Ra) was investigated. It was noted that an increase in pulse duration, peak current, and voltage led to increased roughness. After optimizing the processing parameters (pulse-on time: 0.5 μs , pulse-off time: 16 μs , current: 6 A) based on experimental results, the authors were able to reduce the surface roughness from 4.2 μm (Fig. 4, *a*) to 0.396 μm (Fig. 4, *d*).

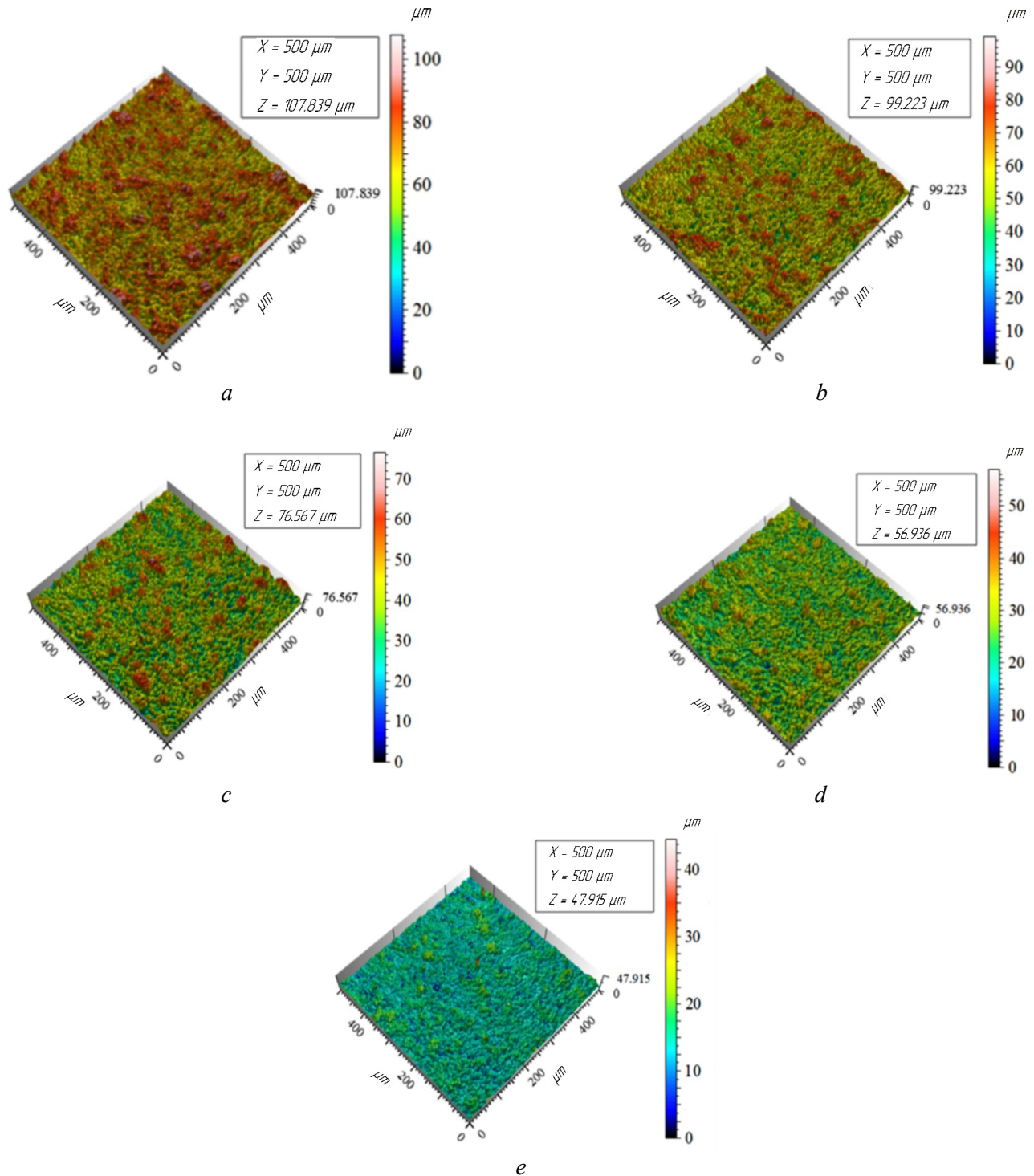


Fig. 4. Surface topography after WEDM of Inconel 718 using:

- a) $T_{on} = 12 \mu\text{s}$, $T_{off} = 0.5 \mu\text{s}$, $I = 12 \text{ A}$; b) $T_{on} = 12 \mu\text{s}$, $T_{off} = 7.5 \mu\text{s}$, $I = 15 \text{ A}$; c) $T_{on} = 4.5 \mu\text{s}$, $T_{off} = 7.5 \mu\text{s}$, $I = 10 \text{ A}$;
 d) $T_{on} = 2 \mu\text{s}$, $T_{off} = 7.5 \mu\text{s}$, $I = 8 \text{ A}$; e) $T_{on} = 0.5 \mu\text{s}$, $T_{off} = 16 \mu\text{s}$, $I = 6 \text{ A}$ [41]

The authors note that the improvement in roughness occurs primarily due to a significant difference between the pulse-on and pulse-off times. It is noted that, compared to other material groups, the machining of heat-resistant materials requires more careful adjustment of processing parameters due to alloying elements and a higher tendency to form intermetallic phases. When machining heat-resistant materials, a lower single pulse energy is employed than when machining other material groups (steels and stainless steels) to achieve low roughness.

EDM process performance

In [42], an experiment was conducted on the material removal rate during *EDM*. The experiments were conducted using three tool electrode materials: copper, graphite, and aluminum. It was found that the graphite electrode demonstrated the highest material removal rate (*MRR*), followed by copper and aluminum electrodes. The graphite electrode also exhibited the lowest wear rate, which is attributed to its high melting point, while the aluminum electrode yielded the best roughness in the experiments. It was noted that when processing heat-resistant materials, non-uniformity of tool electrode wear occurs. This is due to the non-uniform composition of heat-resistant materials and the presence of refractory material inclusions (tungsten, molybdenum), which lead to varying erosion resistance in the machined surface areas. Areas with molybdenum and tungsten are characterized by increased melting thresholds and different thermal conductivity compared to other areas. In contrast, when processing materials from other material groups, such as steel or stainless steel, uniform tool electrode wear and material removal are characteristic, attributed to the homogeneity of the processed material areas.

In [32], it is noted that to achieve minimal tool electrode consumption in the *EDM* process, the lowest peak current and the shortest pulse duration should be employed. In [43], it is noted that the main parameter affecting *EDM* quality is the current, which determines the material removal rate, while the pulse duration is a key indicator primarily influencing tool electrode wear. Studies have shown that an increase in the discharge current of a single pulse leads to a stronger spark and the melting of a larger amount of material per single pulse.

In [44], the authors investigated the effect of inclusions in the working fluid on process productivity. The inclusions used were graphene and multi-walled carbon nanotubes. It was observed that the addition of nanocarbon particles slowed the material removal rate from the workpiece by an average of 15–17%. This effect is associated with an increase in liquid viscosity and a deterioration in sludge removal from the processing zone.

A comparison of the effect of the environment using oil and high-carbon liquid as the working fluid is presented in [45]. The results demonstrated a significant increase in discharge energy density, leading to intensified material removal from the workpiece surface.

The tool electrode material plays an important role in *EDM* process productivity. The main tool electrode materials are presented in Fig. 5.

Recent studies have been conducted on the effect of the tool electrode material on process productivity in [46–47]. It has been established that the copper electrode exhibits a higher material removal rate (up to 10.7 mm³/min) and the lowest tool electrode wear (13–14%). Copper electrodes are used for finishing passes when processing heat-resistant alloys, ensuring high quality of the machined surface with minimal formation of surface defects. Copper tool electrodes

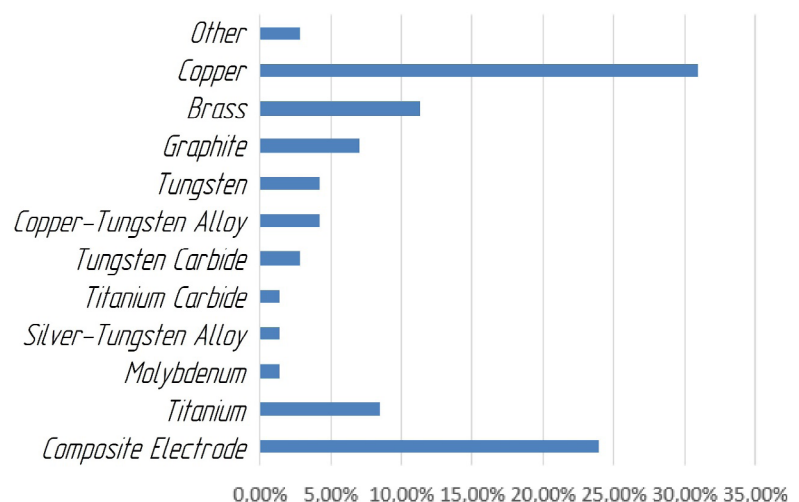


Fig. 5. Types of tool electrode materials used in the *EDM* process

are characterized by high electrical conductivity, which ensures effective electrical current flow, and excellent thermal conductivity, which facilitates rapid heat removal from the processing zone, especially when machining areas containing refractory materials.

Accuracy of the EDM process

In the case of *WEDM* of heat-resistant alloys, one of the key accuracy parameters is the interelectrode gap (*IEG*). The stability of the *WEDM* process depends on the *IEG* value – an increase in the gap leads to uneven pulse energy distribution, resulting in process instability and deviations in geometric dimensions [48].

Fig. 6 shows the results of studies on the cutting width of heat-resistant materials [49–51].

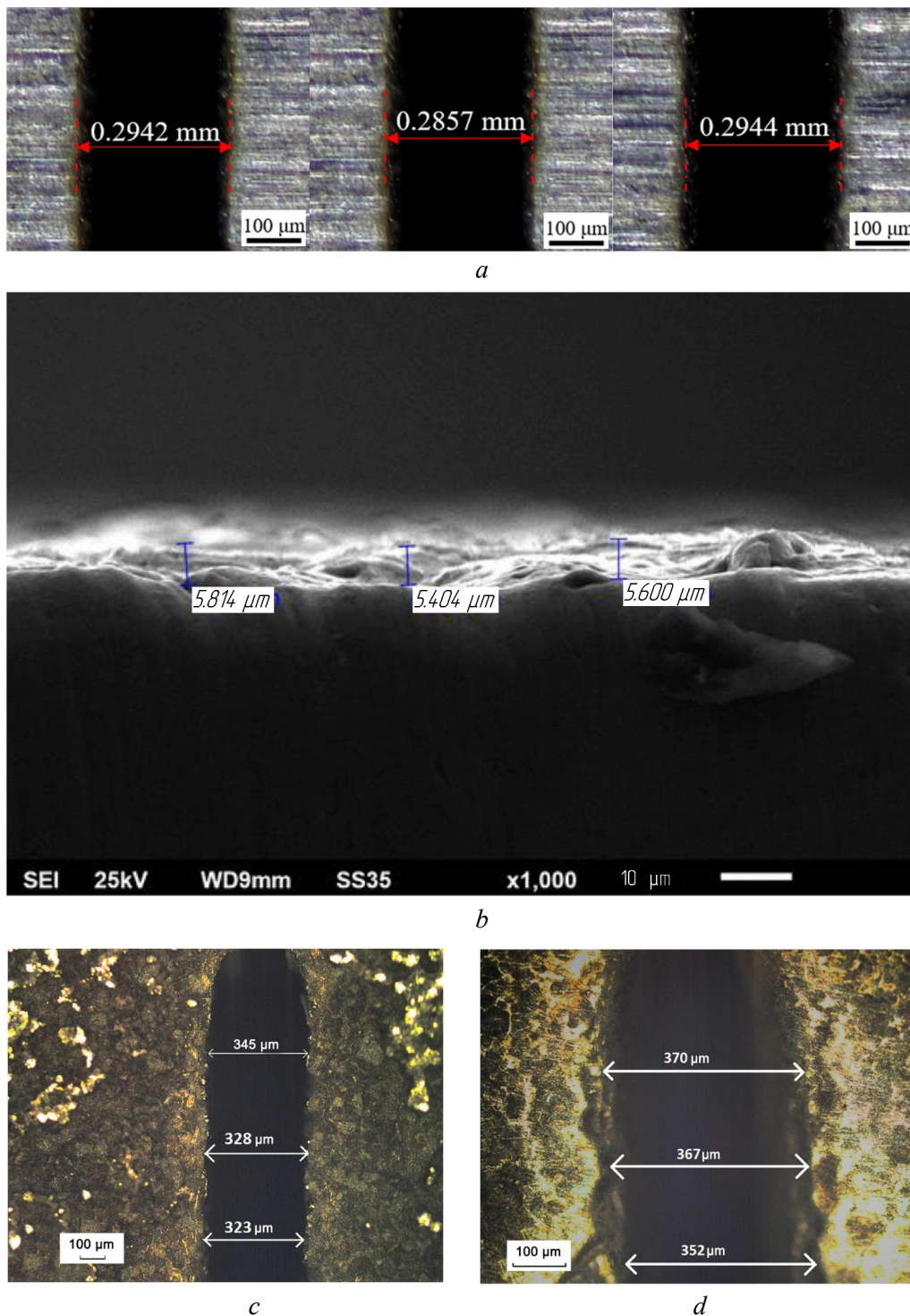


Fig. 6. Investigation of the cutting width in *WEDM*:

a) *Inconel* 718 [49]; b) *Inconel* 617 [50]; c) *VV751P* [51]

The authors of [49–51] investigated the effect of processing parameters—current (I), pulse-on time (t_{on}), and pulse-off time (t_{off})—on the cutting width and the interelectrode gap (IEG) size in *WEDM*, using a 0.25 mm diameter wire as the tool electrode. The developed empirical models indicate that with an increase in current and pulse-on time, single discharge intensity increases, leading to more intense material melting. In [49], the smallest cutting width was obtained at the highest processing power. The authors note that this is attributed to the fact that at higher power, the tool electrode melts the material faster and traverses the machining path more quickly, thereby transferring less thermal energy to the workpiece. The results obtained from these studies enable rationalization of processing parameters and control of the cutting width with minimal thermal impact on the workpiece, thereby minimizing surface defects. A comparative analysis of the results from three independent studies suggests that the results are consistent and demonstrate a high degree of reproducibility under identical electrical discharge machining conditions. The consistency of the output parameter – the cutting width – when machining various heat-resistant materials indicates that the machining parameters are universally applicable to heat-resistant materials, allowing their use for a wide range of such alloys.

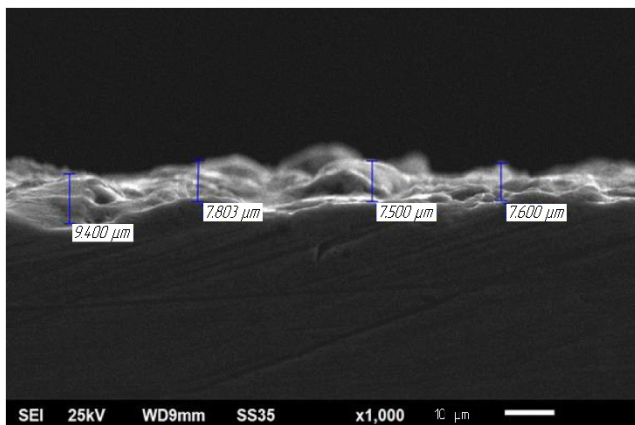
Deformed (white) layer

It has been established that during electrical discharge machining (*EDM*), when removing material in the spark gap between the tool electrode and the workpiece, part of the material is flushed away by the working fluid, while the remaining molten metal re-solidifies and hardens in the presence of a dielectric fluid. This re-solidified material forms the recast layer, often referred to as the white layer. The white layer typically possesses a fine-grained, hard, and brittle microstructure due to local thermal action. As the cooling rate from the surface into the bulk material is very high, a steep thermal gradient is created, influencing the microstructure of this layer. Residual stresses, inherent to the *EDM* process, often lead to the formation of voids and microcracks, which adversely affect the product's operational properties. This layer must be minimized by careful selection of processing parameters due to the presence of voids, micropores, and surface microcracks that can extend deep into the base material. Each material exhibits unique characteristics of white layer formation, which are associated with its operational properties and chemical composition [52–53].

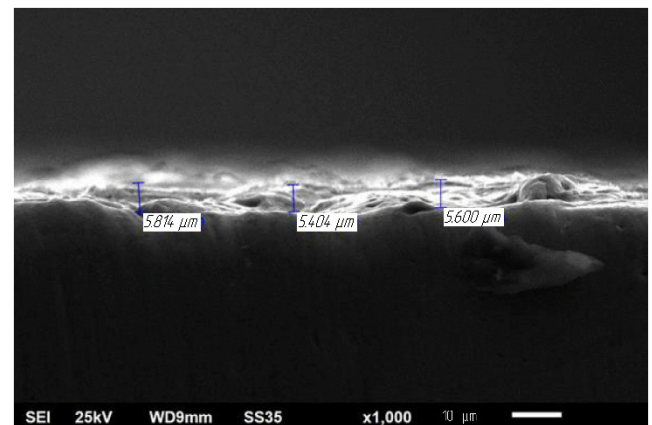
It is noted that there are few studies by research teams investigating the formation and influence of the altered (white) layer during the processing of heat-resistant alloys. This is primarily attributed to the complexity of studying and obtaining high-quality samples for research, as the layer's formation results from intricate and often difficult-to-predict thermal processes. Furthermore, the authors [32, 54] note that the formation of a recast (white) layer on the surface of heat-resistant alloys is affected by numerous factors, including the processing mode, the workpiece material, and the working fluid parameters, which complicates the research process. The authors of these works note that when a white layer forms on heat-resistant materials after processing, a more intense formation of a deformed layer with greater depth is characteristic compared to processing other material groups (e.g., steel or stainless steel). This is attributed to the high heat resistance of the material and its thermal properties. The uneven distribution of the white layer is due to the complex nature of heat-resistant materials, characterized by heterogeneity of both their chemical composition and structural components.

In [55], the authors found that the size of the recast (white) layer during *WEDM* is affected by the processing parameters, namely, the current at constant voltage and the pulse duration. It is noted that when using minimum parameter settings, the size of the white layer is stable and continuous, which is important for post-processing and product operation. In [54], the authors drew attention to the influence of not only the duty cycle but also the polarity on the consistency of the resulting modified layer. It is noted that when using direct polarity, the modified layer is more stable, and the machined surface exhibits a smooth and uniform structure, in contrast to reverse polarity, which is characterized by cracks and craters on the machined surface.

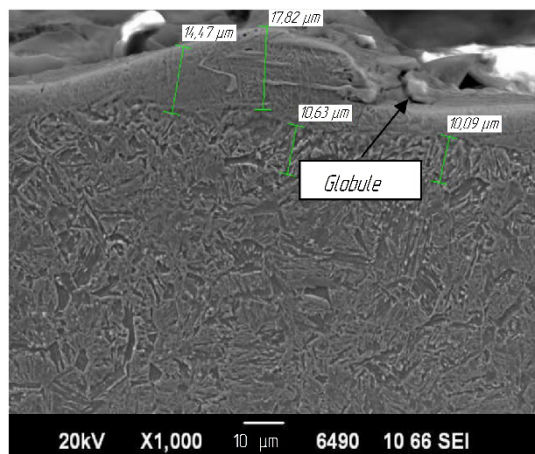
Fig. 7 shows the results of studies by the authors [56–59] on the modified layer during *WEDM* of various heat-resistant materials.



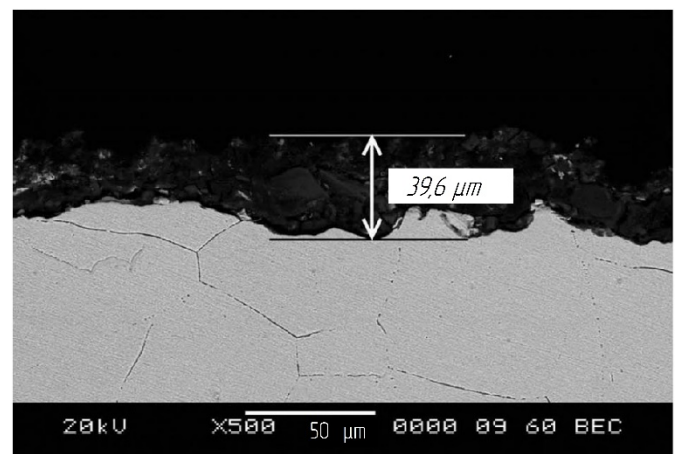
a



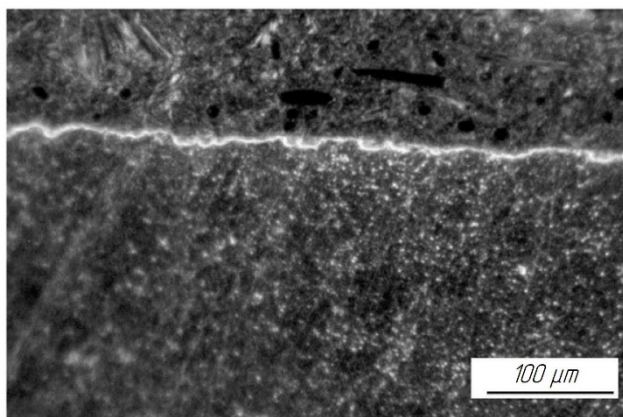
b



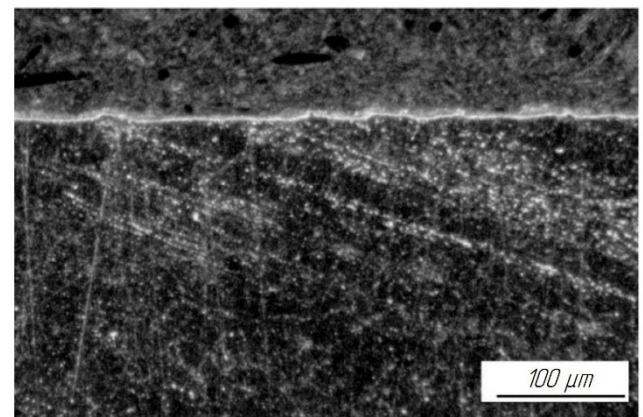
c



d



e



f

Fig. 7. Modifications of the (white) layer on different materials:

a) *Monel 400* (a nickel-copper alloy) [57]; b) *Monel 400* with aluminum powder added to the working fluid [57]; c) high-strength low-alloy steel [56]; d) *Inconel 706* [58]; e) *VV751P* at minimum mode [59]; f) *VV751P* at maximum mode [59]

The authors of [56] conducted a factorial experiment on the recast (white) layer and found (Fig. 7, c) that under a specific processing mode with a pulse-on time of 96 μs , the layer thickness was unevenly formed, measuring 14–17 μm . This was attributed to unstable interelectrode gap conditions and current instability. They also suggested that this layer is formed by molten material not fully removed from the *IEG* zone during processing. In [57], a study investigated the effect of adding aluminum powder to the working fluid on the formation of a recast (white) layer. It was found that the thickness of the white layer using distilled water ranged from 7 to 9 μm (Fig. 7, a), and the addition of aluminum powder to the working fluid had a positive effect, reducing the layer thickness to 5 μm .

In [58], it was established that during WEDM processing of the material, the thickness of the modified layer was $39.6\text{ }\mu\text{m}$ (Fig. 7, g), attributed to the high energy of single pulses in the selected mode. The large thickness of the modified layer led to the formation of numerous microvoids and microcracks and resulted in lower hardness due to thermal alteration of this layer. In [59], studies investigated the influence of WEDM parameters, namely the current intensity and pulse timing, on the formation of the modified layer. It was established that the size of the modified layer was consistently about $10\text{ }\mu\text{m}$ over the entire area (Figs. 7, d and 7, e). In [58, 59], residual stresses in the modified layer were studied. It was established that tensile stresses were observed during the processing of *Inconel 706*, as well as *VV751P*. Residual stresses arise due to significant local thermal impact and can lead to a decrease in the hardness of the surface layer. The relationship between residual tensile stresses and microhardness is discussed in [60].

In [39], the authors investigated the influence of inclusions in the working fluid on the formation of a recast (white) layer. The inclusions used were graphene and multi-walled carbon nanotubes. The authors found that when using graphene during the processing of *Inconel 825*, the thickness of the modified layer was $21.5\text{ }\mu\text{m}$, and when using multi-walled carbon nanotubes, the layer thickness was $29.5\text{ }\mu\text{m}$, which is significantly less than that obtained with conventional processing ($42.21\text{ }\mu\text{m}$). The observed difference in recast layer formation may be attributed to an increased thermal energy transfer rate due to the improved dielectric medium. It is the presence of conductive nanocarbon particles in the dielectric medium that acts as an additional discharge channel, facilitating heat dissipation.

In [40], the authors conducted a study of the influence of the working fluid on the formation of the recast (white) layer. Deionized water was found to be the most effective dielectric, attributed to its lower viscosity and density, which favorably impact multiple discharges in the interelectrode gap and reduce the altered (recast) layer thickness (Fig. 8). This effect is most noticeable when using the maximum power mode (at a current of 9 A): in deionized water, the altered layer thickness was $16\text{ }\mu\text{m}$, compared to $18\text{ }\mu\text{m}$ in kerosene. The altered layer structure obtained with deionized water was also noted to be smoother, lacking sharp phase transitions, whereas in kerosene, individual areas of uneven recast layer distribution were observed. In conclusion, it is worth noting that although kerosene is a common commercial dielectric, the use of deionized water has a favorable effect on surface quality.

In [61], the authors conducted experimental studies to analyze the role of the thermal conductivity of the workpiece material in the electrical discharge machining process. The workpieces used were aluminum, brass, and *Inconel 617*. Under the same machining conditions, a comparatively thicker recast (white) layer ($16\text{ }\mu\text{m}$ – $17.4\text{ }\mu\text{m}$) was formed on aluminum than on brass ($6.4\text{ }\mu\text{m}$ – $8.5\text{ }\mu\text{m}$), while the thinnest recast layer was formed on *Inconel 617* ($1.5\text{ }\mu\text{m}$ – $2.1\text{ }\mu\text{m}$). This phenomenon can be attributed to the fact that materials with lower thermal conductivity struggle to dissipate the heat generated during electrical discharge machining. This results in a localized temperature increase, which in turn contributes to the formation of thinner layers, as the heat becomes concentrated over a smaller area.

Surface quality: cracks and depressions

In [43], it was observed that an increase in the discharge current of a single pulse leads to an intensification of crack formation on the surface of samples and an increase in the thickness of the recast (white) layer.

A modern and promising method for improving surface quality and significantly increasing the productivity of the electrical discharge machining process is powder electrical discharge machining (PEDM). The essence of this technology is that fine particles (metal powders, carbon allotropes) are added to the working fluid. Fine particles dispersed in the liquid form conductive chains within the fluid, thereby enhancing the electrical breakdown efficiency. This enhanced breakdown efficiency leads to an increase in the material removal rate (MRR) from the tool-electrode (TE) surface. The authors of [62–63] found that, upon applying an appropriate voltage, an electric field is created that induces positive and negative charges on the powder particles. These charged particles migrate rapidly in a zigzag pattern, effectively bridging the inter-electrode gap and enhancing the localized electric field strength. This enhanced localized electric field strength, resulting from the reduced effective gap, facilitates efficient inter-electrode breakdown. When the

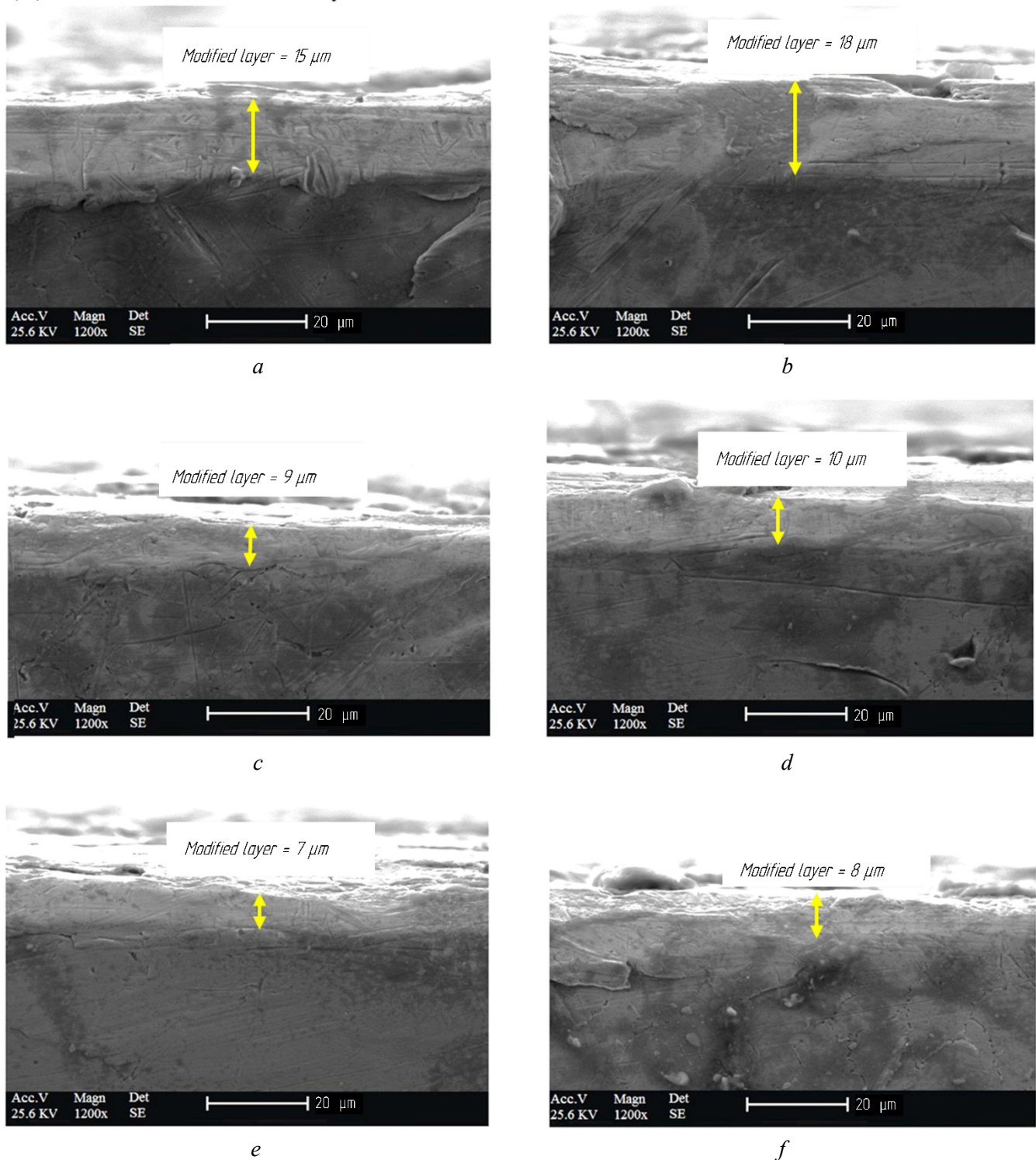


Fig. 8. Modified layer after EDM of AlSi 1045 steel using deionized water as a dielectric:

a) at a current of 9 A and a pulse on-time of 100 μs; b) at a current of 6 A and a pulse on-time of 100 μs; c) at a current of 3 A and a pulse on-time of 100 μs using air; d) at a current of 9 A and a pulse on-time of 100 μs; e) at a current of 6 A and a pulse on-time of 100 μs; f) at a current of 3 A and a pulse on-time of 100 μs [40]

critical breakdown voltage is reached in the region of minimum inter-electrode gap, an electrical discharge occurs, which leads to material removal from the workpiece.

In [64], the author investigated the effect of adding aluminum, chromium, and copper powders to the dielectric fluid on the material removal rate (*MRR*) and tool wear rate during electrical discharge machining. The authors concluded that the particle concentration, particle size, particle density, electrical resistance, and thermal conductivity of the powders play an important role in improving the efficiency of electrical

discharge machining. Proper selection of powder type and concentration can lead to an increased material removal rate and reduced tool wear. Based on the results of the research, the authors concluded that powder with a small particle size can improve both the material removal rate (*MRR*) and the surface quality. However, with a small particle size, a relatively thick recast (white) layer was found, while the thickness of the recast layer decreased as particle size increased. Additionally, silicon powder-mixed electrical discharge machining was employed, with varying powder concentration and flushing rate. It was concluded that the use of a silicon powder-mixed dielectric can significantly improve the surface morphology in terms of reducing the size of craters, obtaining a thin recast layer, and an excellent surface finish. The authors also emphasized that the powder concentration and flushing rate must be carefully selected to improve machining efficiency and surface quality. This is attributed to the significant impact of the working fluid's rheological properties on flushing efficiency in electrical discharge machining. Different types of particles have different effects on the viscosity of the fluid, which, in turn, influences the optimal flushing parameters.

For example, tungsten powder when mixed with the dielectric fluid provides an increased material removal rate and reduces tool electrode wear [65]. Silicon carbide powder dispersed in the dielectric fluid improves surface finish [66] and increases the recast (white) layer thickness [67]. The authors of [68] investigated the inclusion of silicon and chromium powder in the working fluid. The results indicate a significant improvement in the material removal rate and a reduction in tool electrode wear rate. Chromium exhibits high wear resistance and resistance to abrasion, thereby promoting high-quality surface treatment. Its high temperature resistance makes it an ideal candidate for inclusion in the working fluid. Chromium powder mixed with a dielectric fluid improves the material removal rate, reduces tool wear, and the electrode wear ratio.

In [57], the authors noted the positive effect of aluminum powder inclusions on surface morphology, leading to a smoother surface texture with fewer craters and cracks. They explained that cracks are formed due to cavitation shocks that occur when the vapor-gas bubble collapses. These shocks are attributed to significant thermal differences (at the discharge zone, the temperature reaches 10,000 °C, while the working fluid temperature is 20 °C) [43–45].

In [39], the authors investigated the effect of inclusions in the working fluid on surface quality. The inclusions used were graphene and multi-walled carbon nanotubes. They noted that the use of these materials in the working fluid reduces crack formation during processing by 20–25%.

For example, in [57], the authors provide an explanation for the reduction in crack density when adding carbon nanoparticles to the dielectric fluid. According to their research, the addition of microsilicon containing carbon nanopowders improves the thermal conductivity of the dielectric medium, which enhances the rate of heat transfer within the dielectric medium and facilitates heat removal from the *IEG* zone. Consequently, the improved heat transfer rate reduces the energy density in the channel of a single discharge, thereby reducing the crack density on the surface of the samples. Based on this analysis, it is evident that the use of conductive nanoparticles is promising for this industry and requires additional attention from research teams.

The features of the processed surface were investigated by scanning electron microscopy in [69]. It was found that samples processed in a dielectric fluid with added titanium powder had fewer cracks, depressions, and micro-holes, as well as less deposition of material from the working fluid and electrode, compared to samples treated in a medium with added graphite powder. However, this study did not include a comparison with an oil-based dielectric medium. Hydrocarbon-based dielectric fluid is recognized as the most suitable for high-energy single discharges. However, it was also found that the density of defects (cracks and micro-holes) increased with increasing discharge energy. The thickness of the recast layer also increased with increasing fluid viscosity due to inefficient removal of debris from the interelectrode gap zone, which led to re-solidification of the material in the processing zone.

In [70], a study was conducted on the effect of Al_2O_3 inclusions in the working fluid during *EDM* of *Inconel* 825 alloy. The surface characteristics were compared between treatment with Al_2O_3 inclusions in the working fluid and processing in a pure working fluid. The authors note that during conventional *EDM* (i.e., with pure working fluid), many micro-holes, micro-cracks, and material redeposition are concentrated

on the surface, which arise due to uncontrolled deposition of material from the working fluid. In contrast, when Al_2O_3 was added to the working fluid during processing, these defects were largely absent.

In [40], the authors conducted a study of the effect of pulse duration and the type of working fluid on crack formation during machining. They noted that an increase in pulse duration intensifies microcrack formation. This is attributed to the fact that a longer pulse duration leads to an increased energy input into the single discharge zone, which, in turn, raises localized temperatures and the temperature gradient on the processed surface, consequently increasing crack density.

When using kerosene as a working fluid, a greater number of cracks were observed on the surface. Deionized water, due to its distinct discharge characteristics (e.g., more frequent but lower energy discharges), generates lower spark power and discharge energy. Accordingly, lower spark intensity and a reduced temperature gradient on the processed surface result in a lower probability of microcrack formation when machining with deionized water. Another reason for the higher crack density on the processed surface when using kerosene is the difference in thermal conductivity between the two dielectric types, which affects the cooling rate in the discharge zone. The high cooling rate of deionized water effectively dissipates heat from the molten material and limits microcrack formation.

Moreover, during the EDM process with kerosene as a dielectric, carbonization leads to carbon residues adhering to the electrode surface, which eventually results in carbide formation on the workpiece surface. This condition results in unstable machining in the discharge zone, accompanied by increased impulsive forces, which, in turn, leads to a greater tendency for crack propagation during machining with kerosene.

In [71], the authors conducted a comprehensive study of the effect of machining parameters and the addition of carbon nanotubes to the working fluid on crack formation during the machining of Inconel-718 alloy. The machining was carried out at a current of 2 to 8 A. They found that with an increase in the peak current up to 6 A, the density of surface cracks tended to increase. However, with a current ranging from 6 to 8 A, the density of cracks on the processed surface decreased sharply (fig. 9).

This phenomenon may be due to the fact that an increasing peak current removes protruding material particles from the processed surface. However, a further increase in current leads to an intensification of single-pulse discharges and a larger volume of material removal, which, in turn, reduces the flushing efficiency of the dielectric liquid in the interelectrode gap. Upon the termination of discharges, when the electrode retracts to clean the interelectrode gap, due to the large temperature difference, unremoved particles remaining on the surface re-solidify, forming a secondary layer. Subsequently, the machining process is repeated, and the molten material can potentially fill these pores and cracks. Thus, it becomes difficult to assess and detect the presence of surface cracks.

Most studies are aimed at investigating the processed surface with the addition of inclusions, but the issue of the effect of the added powder on the properties of the working medium and the relationship between the change in dielectric properties due to the addition of powder has not been fully studied, as emphasized by the authors of [72]. They compared the addition of a conductive micropowder (graphite) and a non-conductive micropowder (aluminum oxide) to the working fluid (*WF*). The dielectric breakdown voltage values measured for kerosene, a mixture of kerosene with graphite powder, and a mixture of kerosene with aluminum oxide powder were 1,521.74 V, 26 V, and 1,652.17 V, respectively. It was found that the dielectric breakdown voltage is minimal in the presence of graphite powder and maximal in the presence of aluminum oxide powder.

This may be due to the fact that graphite powders possess electrical conductivity, and therefore, when graphite powder is added to a dielectric, its insulating capacity decreases, consequently reducing the dielectric breakdown voltage. Since aluminum oxide powder is not electrically conductive, its addition to a dielectric can increase the dielectric breakdown voltage even more than in the uncontaminated state of the dielectric. It was concluded that the choice of powder additives requires a careful approach, considering not only their effect on the processed surface but also their impact on the dielectric properties of the working medium.

Inclusions in the surface layer after machining

One of the parameters that are difficult to predict is the surface alloying of heat-resistant alloys with tool electrode material particles. This difficulty arises from the fact that it is extremely difficult to develop

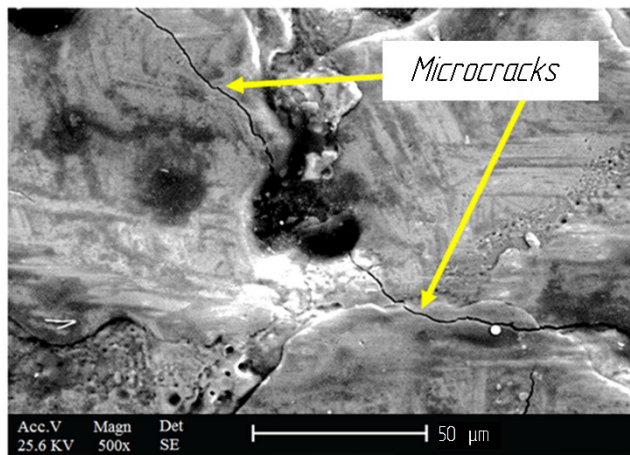
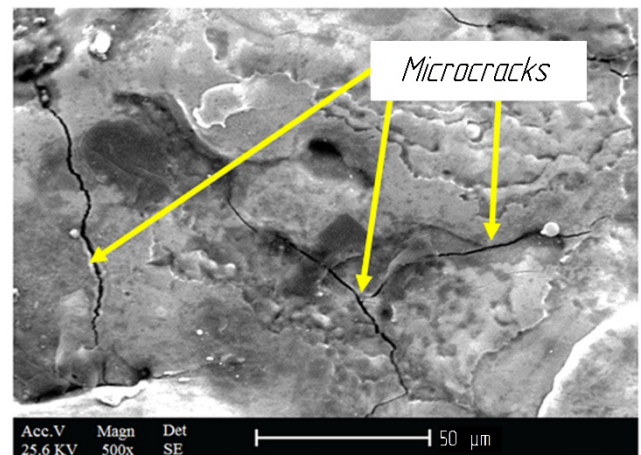
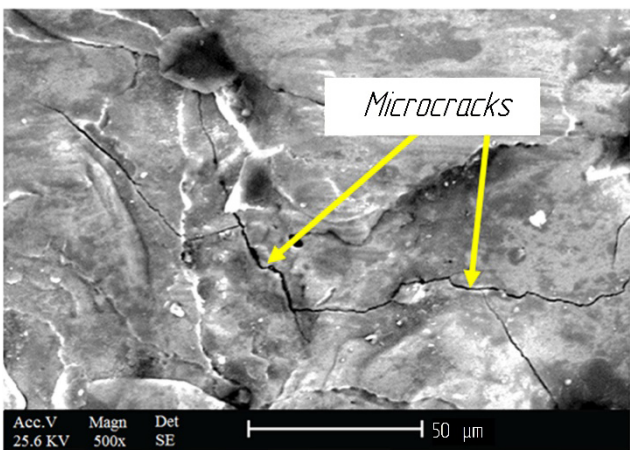
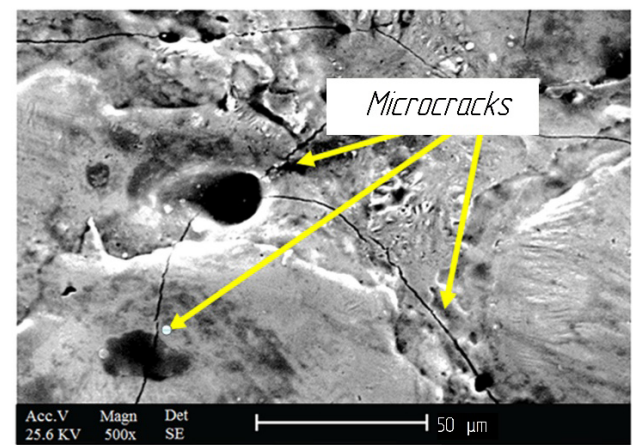
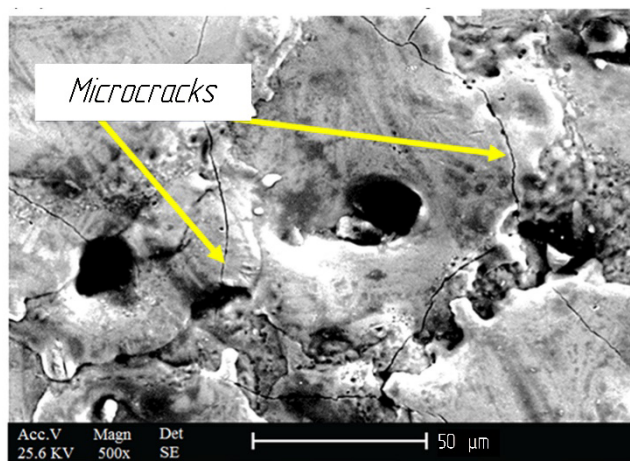
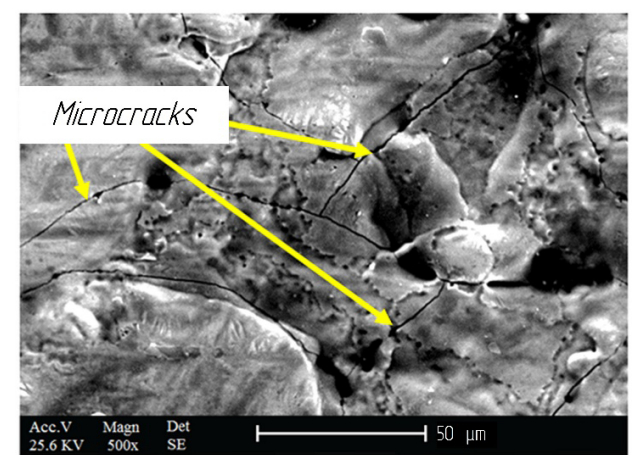
*a**b**c**d**e**f*

Fig. 9. The surface after EDM of AISi 1045 steel using deionized water as a dielectric (*a, c, e*):

a) at a current of 6 A and a pulse on-time of 150 μ s, *c*) at a current of 6 A and a pulse on-time of 100 μ s, *e*) at a current of 6 A and a pulse on-time of 50 μ s and kerosene (*b, d, f*): *b*) at a current of 6 A and a pulse on-time of 150 μ s; *d*) at a current of 6 A and a pulse on-time of 100 μ s, *f*) at a current of 6 A and a pulse on-time of 50 μ s [40]

a mathematical model describing the processes occurring on the machined surface, particularly considering the mass transfer of erosion products. Currently, there is no unified thermodynamic model of the process, nor have fundamental studies been conducted on the formation processes of surface modified layers.

Microstructural changes in the processed surface of heat-resistant materials after EDM are represented by residual electrical discharge machining debris, tool electrode material particles, erosion products, and closed pores containing the working fluid. The mechanical characteristics of the processed surface

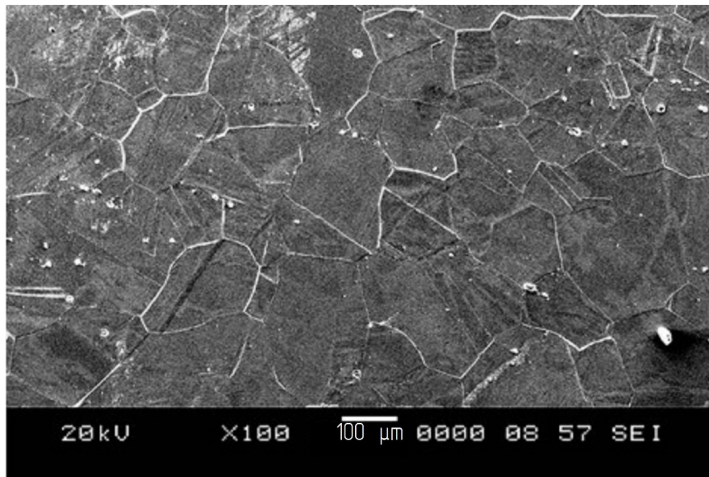


Fig. 10. Inclusions in the surface layer after WEDM of Inconel 706 [44]

appearance of foreign elements not inherent to the original chemical composition – 9 % sodium, 4 % chlorine, and approximately 1 % potassium.

Analysis of point 2, which was located on the recast (white) layer, revealed more significant changes in the main elemental composition of this alloy: a reduction in nickel to 50 %, a 9 % decrease in chromium content, and a 3 % decrease in aluminum. Complete removal of cobalt, molybdenum, tungsten, and vanadium from the surface layer was also observed. This layer was also characterized by the appearance of up to 47 % chlorine and up to 31 % sodium, which is attributed to the use of distilled water as the working fluid. The change in the concentration of alloying elements is associated with the high machining temperature and their solubility in the liquid phase, their migration within the crystallizing material, and the directional crystallization of the recast layer, which collectively accelerate the thermal diffusion of the elements.

In [74], the authors conducted a study of the influence of machining parameters on inclusions in the surface layer and changes in the chemical composition (Fig. 11).

The experiments were conducted across various machining operations, including rough machining, finishing, grinding, and grinding with etching. It was found that the surface after rough WEDM showed the presence of oxygen due to oxidation of various alloying elements. Finishing resulted in a slight 10–12 % decrease in oxygen content on the workpiece surface. The surface layer contained elements such as zinc and copper, which diffused from the tool electrode during machining. The surface obtained by multi-pass cutting exhibited a higher retention of the original alloy elements.

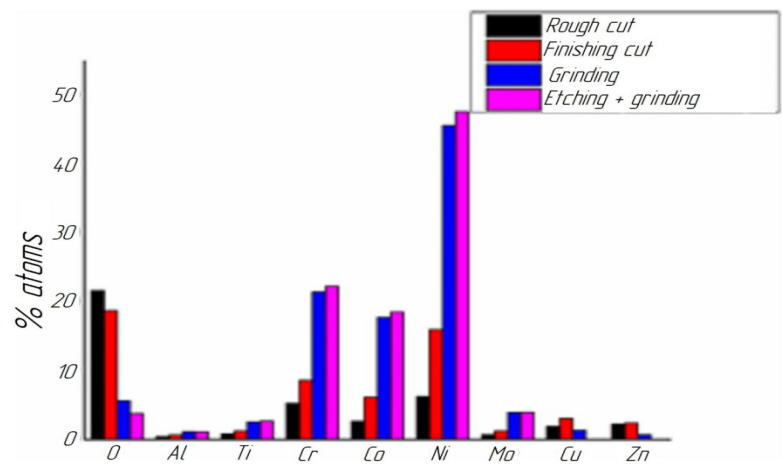


Fig. 11. Inclusions in the surface layer after WEDM of Nimonic C263 material

Influence of tool electrode configuration and material

Scientific studies of the efficiency of the EDM process less extensively investigate the influence of flushing in the interelectrode gap (IEG). The authors of such studies often note the influence of IEG flushing on increasing process productivity and improving surface quality.

In [75–76], the authors designed tool electrodes with internal channels for more efficient removal of debris from the machining zone and enhancing the cooling efficiency of the tool electrode. This resulted in a 40–45% increase in process productivity.

In [77], the authors conducted a comparison of a solid tool electrode and a porous electrode (Fig. 12).

The use of a hollow porous electrode resulted in a three-fold increase in machining efficiency compared to a solid electrode. The machining time was reduced by 47%, which is attributable to better cooling of the tool electrode and a more efficient flow of working fluid.

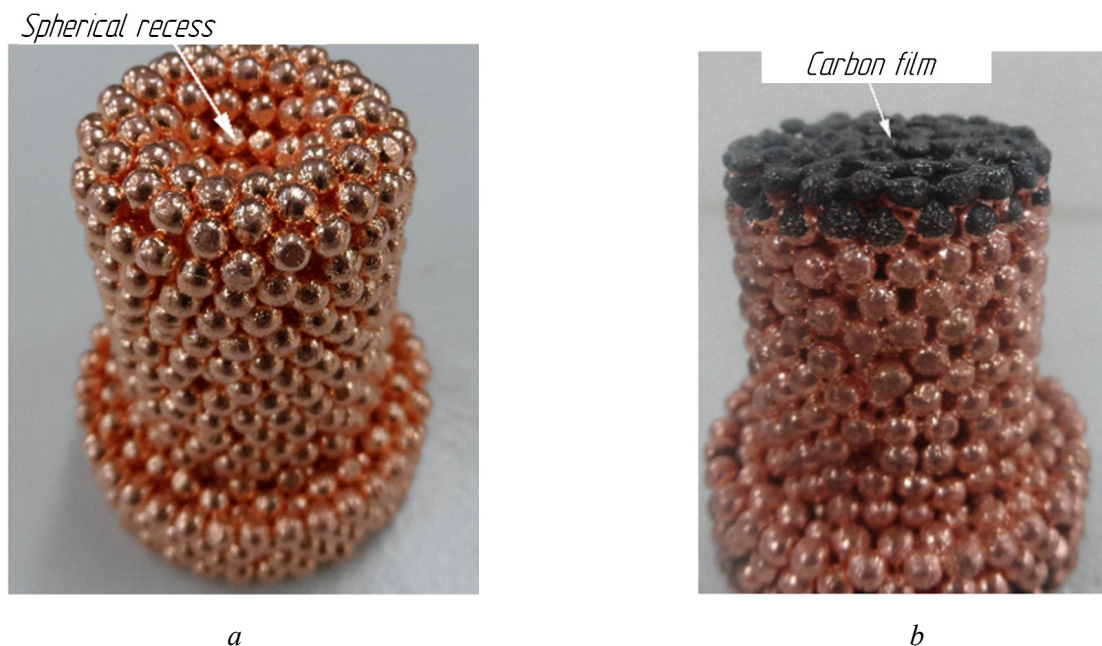


Fig. 12. Copper electrode tool used in EDM :

a) before processing; b) after processing [53]

In [78–79], the authors manufactured tool electrodes using a reinforcing matrix of graphene. The unique properties of graphene (high electrical and thermal conductivity, superior to copper's) make it a promising material for use as a tool electrode in EDM. However, due to the high cost of the material, it is advisable to use it as a reinforcing matrix or as inclusions in the manufacture of tool electrodes. The authors found that the use of composite tool electrodes made it possible to reduce the wear of tool electrodes during machining. This is associated with enhanced heat dissipation in the machining zone and a reduction in the tool electrode temperature experienced during machining. The use of these matrices enables a significant increase in the service life of the tool electrodes.

In [80], the authors conducted research on the use of a spiral tool electrode. The study particularly focused on the removal of debris from the processing zone and the supply of working fluid to the processing zone when machining *Inconel-718*. The electrodes used were cylindrical and spiral tool electrodes (Fig. 13), which were rotated at the same speed during machining.

The efficiency of the spiral electrode in EDM exceeds that of traditional cylindrical electrodes due to the higher axial speed. With an increase in the rotation speed, the maximum axial speed of the spiral electrode increases, thereby significantly increasing the circulation

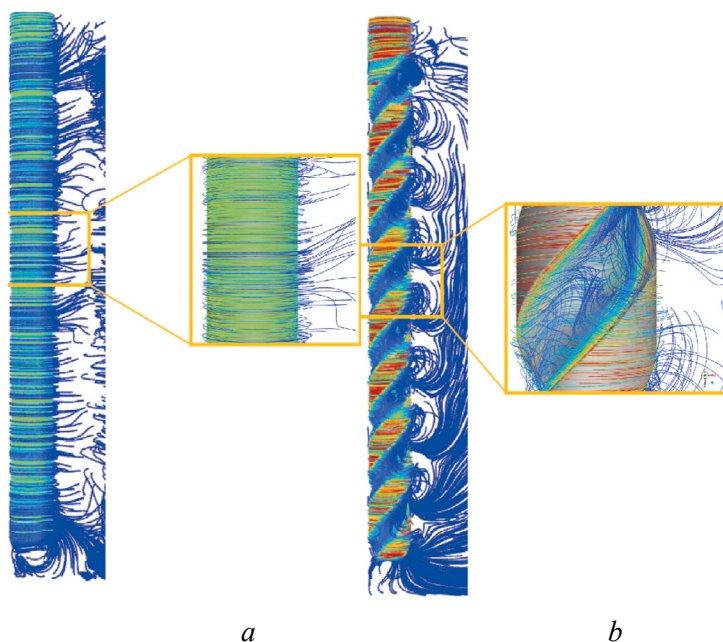


Fig. 13. Axial velocity contours of a) cylindrical and b) spiral tool electrodes [80]

of the working fluid in the machining zone. Additionally, the spiral tool electrode has a lower electrode wear rate than the cylindrical one, which positively impacts the efficiency of using these electrodes.

On the side wall of the slot, the surface roughness of the workpiece machined with the spiral electrode is only 11 μm , which is better than 28 μm of the cylindrical electrode. The spiral electrode shows superiority over the traditional cylindrical electrode in discharge stability, electrode life, slot dimensional accuracy, and surface quality.

Under the same machining conditions, the thickness of the recast layer was reduced from 107.82 μm to 44.37 μm for the spiral electrode compared to the cylindrical electrode process, while in some areas the recast layer was absent.

The analysis shows that the spiral electrode has significant advantages in the debris removal system compared to the cylindrical one. This is due to its design features, which provide more efficient movement and removal of debris particles from the machining zone. The spiral geometry of the electrode creates unique conditions, specifically: the formation of vortex flows of the working fluid, improved circulation of the working fluid in the machining zone, an optimized and ordered trajectory for the removal of debris particles, and the prevention of stagnant zones, which can lead to secondary remelting.

In [81–83], the authors conducted research on micro-electrode erosion drilling using three different electrodes: a solid tungsten carbide cylindrical electrode, a carbide-tipped drill electrode, and a brass tool electrode. After analyzing the results, the authors established that with the use of the cylindrical electrode, a cone was formed at the exit of the through-hole, attributed to inefficient debris removal from the machining zone during electrical discharge drilling. The geometry of the carbide drill, however, improved debris removal from the interelectrode gap, stabilized the temperature in the machining zone, and reduced the machining time. The choice of tool material significantly affects the productivity of electrical discharge machining: brass provides the most accurate micro-holes (with the least wear, overcut, and taper), though it requires extended machining time. Conversely, tungsten carbide provides high wear resistance but results in larger overcut and taper angles with a moderate machining time. Carbide drills provide a balance of wear resistance, machining time, and overcut/taper angles.

In [84–90], the authors investigated the effects of cryogenic treatment of the tool electrode on the quality and efficiency of electrical discharge machining. Based on the results obtained, it was found that the cryogenically treated tool electrode provides superior machining performance (maximum material removal rate and improved surface roughness) compared to a conventional tool electrode. The authors noted an increase in the electrical conductivity of the brass wire during shallow cryogenic treatment. In addition, it was found that the grains became finer.

These results are directly related to the effect of cryogenic treatment on the structural changes in the tool electrode: the formation of a more uniform structure, the elimination of pores and structural defects, and the reduction of internal stresses. Consequently, the wear resistance of the tool electrode is enhanced.

The effect of cryogenic treatment was further investigated by conducting studies of the machinability of electrical discharge machining on *Inconel 601* using cryogenically treated copper as the tool electrode. Tool wear was reduced by 33% by cryogenic treatment compared to untreated copper tools. The work focused on the influence of current, gap voltage, and pulse duration on material removal rate, electrode wear, and surface roughness. It was found that current was the most important control factor.

Conclusions

This paper reviews the current state of research in the field of electrical discharge machining of heat-resistant alloys. It presents current trends and research interests of scientific teams engaged in this area. A literature analysis of experimental studies was conducted, which revealed the lack of generalized and comprehensive research results. *EDM* is a complex process, the outcome of which is influenced by a multitude of factors, and currently, there are no comprehensive technological or recommendation databases for the machining of heat-resistant alloys.

Based on the conducted literature analysis, the following key findings were established:

1. It is relevant to conduct experimental studies on the influence of various material components added to the working fluid to improve surface quality indicators after EDM, and to investigate the impact of alloying the surface layer of heat-resistant materials with these materials.
2. It has been established that the current strength and pulse duration are the main technological parameters determining the quality of the treated surface and the material removal rate. However, exceeding the optimal pulse duration leads to accelerated wear of the tool electrode and excessive melting of the workpiece, which, in turn, leads to difficulty in efficiently removing debris from the interelectrode gap.
3. The efficiency of using a modified working fluid (e.g., containing graphene and carbon nanotubes) for improving surface quality in the machining of heat-resistant materials has been established.
4. It has been established that inclusions in the working fluid have a significant impact on the process parameters and quality of electrical discharge machining. Analysis shows that the correct selection of material and concentration of inclusions can significantly improve the results of the process.
5. It has been established that the geometric parameters of the tool electrode are one of the determining factors influencing the result of electrical discharge machining. Analysis of the literature shows that the correct configuration of the tool electrode can significantly improve the quality and efficiency of the process. A correctly selected tool electrode design ensures more intensive removal of erosion products from the interelectrode gap, which directly affects the quality of the machining.

References

1. Wang X., Wang G., Wang W., Liu X., Liu Y., Jin Y., Zhang Y. Enhancing corrosion resistance of nickel-based alloys: A review of alloying, surface treatments, and environmental effects. *Journal of Alloys and Compounds*, 2025, vol. 1032, pp. 181–195. DOI: 10.1016/j.jallcom.2025.181014.
2. Li H., Liu H., Li J., Yao H. High-temperature corrosion resistance of weld overlay In625 coating in aggressive environments of waste incinerators. *Corrosion Science*, 2025, vol. 249. DOI: 10.1016/j.corsci.2025.112865.
3. Madhusudan S., Epifano E., Favergeon J., Sanviemvongsak T., Marechal D., Monceau D. High temperature intergranular oxidation of nickel based superalloy Inconel 718. *High Temperature Corrosion of Materials*, 2024, vol. 101, pp. 873–884. DOI: 10.1007/s11085-024-10260-z.
4. Karmuhilan M., Kumanan S. A review on additive manufacturing processes of Inconel 625. *Journal of Materials Engineering and Performance*, 2022, vol. 31, pp. 2583–2592. DOI: 10.1007/s11665-021-06427-3.
5. Pendokhare D., Chakraborty S. A review on multi-objective optimization techniques of wire electrical discharge machining. *Archives of Computational Methods in Engineering*, 2025, vol. 32, pp. 1797–1839. DOI: 10.1007/s11831-024-10195-3.
6. Badoniya P., Srivastava M., Jain P.K., Rathee S. A state-of-the-art review on metal additive manufacturing: milestones, trends, challenges and perspectives. *Journal of the Brazilian Society of Mechanical Sciences and Engineering*, 2024, vol. 46 (6), pp. 339–351. DOI: 10.1007/s40430-024-04917-8.
7. Hasan M.M., Saleh T., Sophian A., Rahman M.A., Huang T., Ali M.S. Experimental modeling techniques in electrical discharge machining (EDM): A review. *The International Journal of Advanced Manufacturing Technology*, 2023, vol. 127, pp. 2125–2150. DOI: 10.1007/s00170-023-11603-x.
8. Ajay P., Dabhade V.V. Heat treatments of Inconel 718 nickel-based superalloy: A review. *Metals and Materials International*, 2025, vol. 31, pp. 1204–1231. DOI: 10.1007/s12540-024-01812-8.
9. Zhou N., Lv D.C., Zhang H.L., McAllister D., Zhang F., Mills M.J., Wang Y. Computer simulation of phase transformation and plastic deformation in IN718 superalloy: Microstructural evolution during precipitation. *Acta Materialia*, 2014, vol. 65, pp. 270–286. DOI: 10.1016/j.actamat.2013.10.069.
10. Lv D.C., McAllister D., Mills M.J., Wang Y. Deformation mechanisms of D022 ordered intermetallic phase in superalloys. *Acta Materialia*, 2016, vol. 118 (1), pp. 350–361. DOI: 10.1016/j.actamat.2016.07.055.
11. Sonar T., Balasubramanian V., Malarvizhi S., Venkateswaran T., Sivakumar D. An overview on welding of Inconel 718 alloy – Effect of welding processes on microstructural evolution and mechanical properties of joints. *Materials Characterization*, 2021, vol. 174, pp. 1–22. DOI: 10.1016/j.matchar.2021.110997.
12. Erdoğan N.N., Başıyigit A.B. Investigating thermal shock and corrosion resistance of Inconel 601 super alloy after thermal barrier coating with %8 YSZ powder. *Materials Today Communications*, 2023, vol. 36, pp. 1–14. DOI: 10.1016/j.mtcomm.2023.106516.

13. Kang H.S., Kim H., Yoon E.Y., Lee Y.S., Kim S., Kim J.G. Re-heat treatment effect on the microstructure and mechanical properties of the Inconel 706 alloy for repair. *Journal of Materials Research and Technology*, 2024, vol. 31, pp. 2193–2201. DOI: 10.1016/j.jmrt.2024.07.011.
14. Mao J., Li X., Bao S., Ge R., Yan L. The experimental and numerical studies on multiaxial creep behavior of Inconel 783 at 700 °C. *International Journal of Pressure Vessels and Piping*, 2019, vol. 173, pp. 133–146. DOI: 10.1016/j.ijpvp.2019.05.005.
15. Jiang R., Mostafaei A., Pauza J., Kantzos C., Rollett A.D. Varied heat treatments and properties of laser powder bed printed Inconel 718. *Materials Science and Engineering: A*, 2019, vol. 755, pp. 170–180. DOI: 10.1016/J.MSEA.2019.03.103.
16. Jamil M.F., Sahto M.P., Mehmood A. Comprehensive study on high-performance machining (HPM) of Inconel-718: a review. *The International Journal of Advanced Manufacturing Technology*, 2025, vol. 139 (11–12), pp. 5305–5337. DOI: 10.1007/s00170-025-16225-z.
17. Bazyleva O.A., Arginbaeva E.G., Shestakov A.V. Zharoprochnye intermetallidnye nikelovye splavy dlya dvigatelei letatel'nykh apparatov [High-temperature intermetallic nickel alloys for aircraft engines]. *Idei i novatsii = Ideas and Innovations*, 2020, vol. 8, no. 3–4, pp. 138–146. DOI: 10.48023/2411-7943_2020_8_3_4_138.
18. Gromov V.I., Yakusheva N.A., Vostrikov A.V., Cherkashneva N.N. Vysokoprochnye konstruktsionnye stali dlya valov gazoturbinnnykh dvigatelei (obzor) [High strength structural steels for gas turbine engine shafts (review)]. *Aviatsionnye materialy i tekhnologii = Aviation Materials and Technologies*, 2021, vol. 62, iss. 1, pp. 3–12. DOI: 10.18577/2713-0193-2021-0-1-3-12.
19. Kuznetsov V.P., Lesnikov V.P., Popov N.A. *Struktura i svoistva zharoprochnykh nikelovykh splavov* [Structure and properties of heat-resistant nickel alloys]. Yekaterinburg, Ural University Publ., 2016. 164 p.
20. Sudhir, Sehgal A.K., Nain S.S. Machine learning algorithms evaluation and optimization of WEDM of nickel based super alloy: A review. *Materials Today: Proceedings*, 2022, vol. 50 (5), pp. 1793–1798. DOI: 10.1016/j.matpr.2021.09.202.
21. Abhilash P.M., Chakradhar D. Prediction and analysis of process failures by ANN classification during wire-EDM of Inconel 718. *Advanced Manufacturing*, 2020, vol. 8, pp. 519–536. DOI: 10.1007/s40436-020-00327-w.
22. Paturi U.M.R., Cheruku S., Pasunuri V.P.K., Salike S., Reddy N.S., Cheruku S. Machine learning and statistical approach in modeling and optimization of surface roughness in wire electrical discharge machining. *Machine Learning with Applications*, 2021, vol. 6. DOI: 10.1016/j.mlwa.2021.100099.
23. Manikandan N., Raju R., Narasimhamu K.L., Damodaram A.K. Optimization of wire electrical discharge machining of Monel 400 using Taguchi-Grey approach. *Materials Today: Proceedings*, 2022, vol. 68 (5), pp. 1690–1696. DOI: 10.1016/j.matpr.2022.08.215.
24. Manikandan N., Binoj J.S., Thejasree P., Abhishek H., Goud B.K. Multi aspects optimization on spark erosion machining of Incoloy 800 by Taguchi Grey approach. *Materials Today: Proceedings*, 2021, vol. 39 (1), pp. 148–154. DOI: 10.1016/j.matpr.2020.06.403.
25. Goyal A. Investigation of material removal rate and surface roughness during wire electrical discharge machining (WEDM) of Inconel 625 super alloy by cryogenic treated tool electrode. *Journal of King Saud University – Science*, 2017, vol. 29, pp. 528–535. DOI: 10.1016/j.jksus.2017.06.005.
26. Archana G., Dharma K.D., Venkataramaiah P. Study on machining response in wire EDM of Inconel 625. *International Journal of Applied Engineering Research*, 2018, vol. 13 (21), pp. 15270–15277.
27. Tata N., Pacharu R.K., Devarakonda S.K. Multi response optimization of process parameters in wire-cut EDM on INCONEL 625. *Materials Today: Proceedings*, 2021, vol. 47 (19), pp. 6960–6964. DOI: 10.1016/j.matpr.2021.05.214.
28. Tondy H.R., Tigga A.M. Empirical assessment and modeling of MRR and surface roughness acquired from wire electrical discharge machining of Inconel 718. *International Journal of Mechanical Engineering and Technology*, 2017, vol. 8 (1), pp. 152–159.
29. Sinha A., Majumder A., Gupta K. A RSM based MOGOA for process optimization during WEDM of Inconel 625. *Proceedings of the Institution of Mechanical Engineers, Part E: Journal of Process Mechanical Engineering*, 2022, vol. 236 (5), pp. 1824–1832. DOI: 10.1177/09544089221074837.
30. Biswas S., Paul A.R., Dhar A.R., Singh Y., Mukherjee M. Multi-material modeling for wire electro-discharge machining of Ni-based superalloys using hybrid neural network and stochastic optimization techniques. *CIRP Journal of Manufacturing Science and Technology*, 2023, vol. 41, pp. 350–364. DOI: 10.1016/j.cirpj.2022.12.005.
31. Shlykov E.S., Ablyaz T.R., Blokhin V.B., Osinnikov I.V., Muratov K.R. Povyshenie effektivnosti elektroerozionnoi obrabotki izdelii, vypolnennykh iz granulirovannogo zharoprochnogo nikelovogo splava VV751P [Increasing the efficiency of electrical discharge machining of products made of granulated heat-resistant nickel alloy]

VV751P]. *Konstruktsii iz kompozitsionnykh materialov = Composite Materials Constructions*, 2025, no. 1 (177), pp. 27–30. DOI: 10.52190/2073-2562_2025_1_27.

32. Said A., Lajis M.A. An electrical discharge machining (EDM) of Inconel 718 by using copper electrode at higher peak current and pulse duration. *Conference Series: Materials Science and Engineering*, 2016, vol. 15 (5), pp. 1–7.

33. Tsai H.C., Yan B.H., Huang F.Y. The properties and characteristics of the new electrodes based on Cr-Cu for EDM machines. *International Journal of Machine Tools & Manufacture*, 2003, vol. 43 (3), pp. 245–252.

34. Zhang J.J., Jiang K.Y., Yan J., Wang F., Wang X.W. Performance and microstructure of TiN/Cu EDM electrodes. *Applied Mechanics and Materials*, 2012, vol. 268, pp. 82–86. DOI: 10.4028/www.scientific.net/AMM.268-270.82.

35. Rajyalakshmi G. Optimization of process parameters of wire electrical discharge machining on Inconel825 using grey relational analysis coupled with principle component analysis. *International Journal of Applied Engineering Research*, 2013, vol. 8 (11), pp. 1294–1314.

36. Jay M., Çaydas U., Hasçalık A. Optimization of micro-EDM drilling of Inconel 718 superalloy. *International Journal of Advanced Manufacturing Technology*, 2013, vol. 66 (5), pp. 1015–1023. DOI: 10.1007/s00170-012-4385-8.

37. Baldin V., Baldin C.R.B., Machado A.R., Amorim F.L. Machining of Inconel 718 with a defined geometry tool or by electrical discharge machining. *Journal of the Brazilian Society of Mechanical Sciences and Engineering*, 2020, vol. 42 (5), pp. 1–14. DOI: 10.1007/s40430-020-02358-7.

38. Mohanty A., Talla G., Gangopadhyay S. Experimental investigation and analysis of EDM characteristics of Inconel 825. *Materials and Manufacturing Processes*, 2014, vol. 29, pp. 540–459. DOI: 10.1080/10426914.2014.901536.

39. Chen N., Kong L., Lei W., Qiu R. Experimental study on EDM of CFRP based on graphene aqueous solution. *Materials and Manufacturing Processes*, 2023, vol. 38 (9), pp. 1180–1189. DOI: 10.1080/10426914.2023.2165674.

40. Rahimi H., Masoudi S., Tolouei-Rad M. Experimental investigation of the effect of EDM parameters and dielectric type on the surface integrity and topography. *The International Journal of Advanced Manufacturing Technology*, 2022, vol. 118, pp. 1767–1778. DOI: 10.1007/s00170-021-08040-z.

41. Sun L., Shi S., Li X., Hou Y., Chu Z., Chen B. Surface microstructure evolution and mechanical property investigation of Inconel 718 alloy using multiple trimmings and WEDM. *Experimental Techniques*, 2025, vol. 49, pp. 299–312. DOI: 10.1007/s40799-024-00749-2.

42. Hasçalık A., Caydas U. Electrical discharge machining of titanium alloy (Ti–6Al–4V). *Applied Surface Science*, 2007, vol. 253, pp. 9007–9016. DOI: 10.1016/j.apsusc.2007.05.031.

43. Mohanty C.P., Mahapatra S.S., Singh M.R. An experimental investigation of machinability of Inconel 718 in electrical discharge machining. *Procedia Materials Science*, 2014, vol. 6, pp. 605–611. DOI: 10.1016/j.mspro.2014.07.075.

44. Talla G., Gangopadhyay S., Biswas C.K. Influence of graphite powder mixed EDM on the surface integrity characteristics of Inconel 625. *Particulate Science and Technology*, 2016, vol. 35 (2), pp. 219–226. DOI: 10.1080/02726351.2016.1150371.

45. Paswan K., Pramanik A., Chattopadhyaya S., Khan A.M., Singh S. An analysis of machining response parameters, crystalline structures, and surface topography during EDM of die-steel using EDM oil and liquid based viscous dielectrics: a comparative analysis of machining performance. *Arabian Journal for Science and Engineering*, 2023, vol. 48 (1), pp. 1–17. DOI: 10.1007/s13369-023-07626-x.

46. Sonker P.K., Nahak B., Singh T.J. Comparative study of copper and graphite electrodes performance in Electrical Discharge Machining (EDM) of die steel. *Materials Today: Proceedings*, 2022, vol. 68, pp. 167–170. DOI: 10.1016/j.matpr.2022.07.182.

47. Singh G., Mahajan A., Devgan S., Sidhu S.S. Comparison of copper and tungsten electrodes for the electric discharge machined SUS-316L. *Sustainable Machining Strategies for Better Performance: Select Proceedings of SMSBP 2020*. Springer, 2022, pp. 197–206. DOI: 10.1007/978-981-16-2278-6_17.

48. Khayrulin V.T., Ablyaz T.R., Shlykov E.S., Blokhin V.B., Muratov K.R. Issledovanie vliyaniya rezhimov protsessa provolochno-vyreznoi elektroerozionnoi obrabotki na formirovanie znacheniya shiriny reza pri obrabotke zharoprochnogo nikelvogo splava VV751P [Study of the influence of wire-cut electrical discharge machining process modes on the formation of the cut width value when processing heat-resistant nickel alloy VV751P]. *STIN = Russian Engineering Research*, 2024, no. 6, pp. 27–30. (In Russian).

49. Sun L., Chu Z., Hou Y., Rajurkar K., Li X., Shi S. Utilizing wire electrical discharge machining for surface quality and precise profile control of Inconel 718 fir-tree slot. *The International Journal of Advanced Manufacturing Technology*, 2024, vol. 133, pp. 1271–1283. DOI: 10.1007/s00170-024-13826-y.
50. Dzionk S., Siemiatkowski M.S. Studying the effect of working conditions on WEDM machining performance of super alloy Inconel 617. *Machines*, 2020, vol. 8 (3), pp. 1–18. DOI: 10.3390/machines8030054.
51. Khairulin V.T., Ablyaz T.R., Shlykov E.S., Blokhin V.B., Muratov K.R. Factors affecting the cut width in the wire-cut electrical discharge machining of VV751P heat-resistant nickel alloy. *Russian Engineering Research*, 2024, vol. 44 (7), pp. 1014–1016. DOI: 10.3103/S1068798X24701387.
52. Padhi P.C., Routara B.C. Effect of recast layer thickness of high-carbon alloy (EN-31) in wire EDM process by varying operating parameters. *Recent Advances in Thermofluids and Manufacturing Engineering: Select Proceedings of ICTMS 2022*. Springer, 2022, pp. 505–517. DOI: 10.1007/978-981-19-4388-1_43.
53. Walder G., Richard J. Removal of the heat affect zone created by EDM with pico-second LASER machining. *Procedia CIRP*, 2016, vol. 42, pp. 475–480. DOI: 10.1016/j.procir.2016.02.235.
54. Ji R., Liu Y., Diao R., Xu C., Li X., Cai B., Zhang Y. Influence of electrical resistivity and machining parameters on electrical discharge machining performance of engineering ceramics. *PLoS ONE*, 2017, vol. 9 (11), pp. 1–9. DOI: 10.1371/journal.pone.0110775.
55. Ablyaz T.R., Shlykov E.S., Osinnikov I.V., Muratov K.R., Khayrullin V.T. Issledovanie mikrostruktury poverkhnostnogo sloya zharoprochnykh materialov, obrabotannykh metodom elektroerozionnoi obrabotki [Study of the microstructure of the surface layer of heat-resistant materials processed by electrical discharge machining]. *STIN = Russian Engineering Research*, 2024, no. 6, pp. 33–35. (In Russian).
56. Azam M., Jahanzaib M., Abbasi J.A., Abbas M., Wasim A., Hussain S. Parametric analysis of recast layer formation in wire-cut EDM of HSLA steel. *The International Journal of Advanced Manufacturing Technology*, 2016, vol. 87, pp. 713–722. DOI: 10.1007/s00170-016-8518-3.
57. Rohilla V.K., Goyal R., Kumar A., Singla Y.K., Sharma N. Surface integrity analysis of surfaces of nickel-based alloys machined with distilled water and aluminium powder-mixed dielectric fluid after WEDM. *The International Journal of Advanced Manufacturing Technology*, 2021, vol. 116, pp. 2467–2472. DOI: 10.1007/s00170-021-07610-5.
58. Sharma P., Chakradhar D., Narendranath S. Analysis and optimization of WEDM performance characteristics of Inconel 706 for aerospace application. *Silicon*, 2018, vol. 10, pp. 921–930. DOI: 10.1007/s12633-017-9549-6.
59. Ablyaz T.R., Shlykov E.S., Blokhin V.B., Osinnikov I.V., Khayrulin V.T., Muratov K.R. Issledovanie vliyaniya rezhimov elektroerozionnoi obrabotki na ekspluatatsionnye svoistva izdelii, vypolnennykh iz granulirovannogo zharoprochnogo nikelovogo splava VV751P [Investigation of the influence of electrical discharge machining modes on operational properties of products made of granulated heat-resistant nickel alloy VV751P]. *Konstruktsii iz kompozitsionnykh materialov = Composite Materials Constructions*, 2024, vol. 2 (174), pp. 22–27. DOI: 10.52190/2073-2562_2024_2_22.
60. Sharma R.K., Singh J. Determination of multi-performance characteristics for powder mixed electric discharge machining of tungsten carbide alloy. *Proceedings of the Institution of Mechanical Engineers, Part B: Journal of Engineering Manufacture*, 2016, vol. 230 (2), pp. 303–315. DOI: 10.1177/0954405414554017.
61. Paswan K., Sharma S., Li C., Mohammed K.A., Kumar A., Abbas M., Tag-Eldin E.M. Unravelling the analysis of electrical discharge machining process parameters, microstructural morphology, surface integrity, recast layer formation, and material properties: A comparative study of aluminum, brass, and Inconel 617 materials. *Journal of Materials Research and Technology*, 2023, vol. 27, pp. 7713–7729. DOI: 10.1016/j.jmrt.2023.11.186.
62. Bui V.D., Mwangi J.W., Schubert A. Powder mixed electrical discharge machining for antibacterial coating on titanium implant surfaces. *Journal of Manufacturing Processes*, 2019, vol. 44, pp. 261–270. DOI: 10.1016/j.jmapro.2019.05.032.
63. Besinis A., Hadi S.D., Le H.R., Tredwin C., Handy R.D. Antibacterial activity and biofilm inhibition by surface modified titanium alloy medical implants following application of silver, titanium dioxide and hydroxyapatite nanocoatings. *Nanotoxicology*, 2017, vol. 11 (3), pp. 327–338. DOI: 10.1080/17435390.2017.1299890.
64. Kumar S., Dhingra A.K., Kumar S. Parametric optimization of powder mixed electrical discharge machining for nickel-based superalloy inconel-800 using response surface methodology. *Mechanics of advanced materials and modern processes*, 2017, vol. 7 (3). DOI: 10.1186/s40759-017-0022-4.
65. Kumar N., Ahsan R. Study of PMEDM efficiency on EN-31 steel using tungsten powder in dielectric fluid. *International Journal of Emerging Technologies in Engineering Research*, 2017, vol. 5 (5), pp. 17–24.
66. Bhaumik M., Maity K. Effect of machining parameter on the surface roughness of AISI 304 in silicon carbide powder mixed EDM. *Decision Science Letters*, 2017, vol. 6 (3), pp. 261–268. DOI: 10.5267/j.dsl.2016.12.004.

67. Al-Khazraji A.N., Amin S.A., Ali S.M. The effect of SiC powder mixing electrical discharge machining on white layer thickness, heat flux and fatigue life of AISI D2 die steel. *Engineering Science and Technology, an International Journal*, 2016, vol. 19 (3), pp. 1400–1415. DOI: 10.1016/j.jestch.2016.01.014.
68. Kazi F., Waghmare C.A., Sohani M.S. Multi-objective optimization of machining parameters in hybrid powder-mixed EDM process by response surface methodology and normalized fuzzy logic algorithm. *The International Journal on Interactive Design and Manufacturing*, 2021, vol. 15, pp. 695–706. DOI: 10.1007/s12008-021-00788-8.
69. Bhowmick S., Paul A., Biswas N., Sarkar S., Majumdar G. Synthesis and characterization of titanium and graphite powder mixed electric discharge machining on Inconel 718. *Advances in Transdisciplinary Engineering*, 2022, vol. 27, pp. 58–63. DOI: 10.3233/ATDE220722.
70. Kumar A., Mandal A., Dixit A.R., Kumar A., Kumar S., Ranjan R. Comparison in the performance of EDM and NPMEDM using Al_2O_3 nanopowder as an impurity in DI water dielectric. *The International Journal of Advanced Manufacturing Technology*, 2019, vol. 100, pp. 1327–1339. DOI: 10.1007/s00170-018-3126-z.
71. Kumar S.B., Saurav D., Mahapatra S.S. On electro-discharge machining of Inconel 718 super alloys: An experimental investigation. *Materials Today: Proceedings*, 2018, vol. 5, pp. 4861–4869. DOI: 10.1016/j.matpr.2017.12.062.
72. Sahu D.R., Kumar V., Mandal A. Surface integrity analysis in powder mixed EDM of Nimonic 263. *Materials Today: Proceedings*, 2022, vol. 62 (1), pp. 353–359. DOI: 10.1016/j.matpr.2022.03.467.
73. Ablyaz T.R., Shlykov E.S., Osinnikov I.V., Blokhin V.B., Muratov K.R. Elektronno-mikroskopicheskii analiz poverkhnostnogo sloya izdelii iz zharoprochnykh nikelevykh splavov posle elektroerozionnoi obrabotki [Electron-microscopic analysis of the surface layer of products made of heat-resistant nickel alloys after electrical discharge machining]. *STIN = Russian Engineering Research*, 2025, no. 5, pp. 55–58. (In Russian).
74. Mandal A., Dixit A.R., Chattopadhyaya S., Paramanik A., Hloch S., Królczyk G. Improvement of surface integrity of Nimonic C 263 super alloy produced by WEDM through various post-processing techniques. *The International Journal of Advanced Manufacturing Technology*, 2017, vol. 93, pp. 433–443. DOI: 10.1007/s00170-017-9993-x.
75. Nguyen H.P., Ngo N.V., Nguyen C.T. Study on multi-objects optimization in EDM with nickel coated electrode using Taguchi-AHP-Topsis. *International Journal of Engineering*, 2022, vol. 35 (2), pp. 276–282. DOI: 10.5829/ije.2022.35.02b.02.
76. Bozdana A.T., Alkarkhi N.K. Comparative experimental investigation and gap flow simulation in electrical discharge drilling using new electrode geometry. *International Journal of Mechanical Sciences*, 2017, vol. 8 (2), pp. 289–298. DOI: 10.5194/ms-8-289-2017.
77. Jiang Y., Kong L., Yu J., Hua C., Zhao W. Experimental research on preparation and machining performance of porous electrode in electrical discharge machining. *Journal of Mechanical Science and Technology*, 2022, vol. 36 (12), pp. 6201–6215. DOI: 10.1007/s12206-022-1134-2.
78. Mondal S., Paul G., Mondal S.C., Mondal K., Seikh Z., Sekh M. Fabrication of graphene reinforced aluminium metal matrix composites for advanced tool materials. *Journal of the Institution of Engineers (India): Series D*, 2024. DOI: 10.1007/s40033-024-00847-w.
79. Mondal S., Paul G., Mondal K., Mondal S.C. Electric discharge machining with graphene reinforced aluminium metal matrix composite (Gr Al MMC) tool for EN 31 die steel work piece. *The Journal of the Institution of Engineers (India): Series C*, 2025, vol. 106, pp. 541–551. DOI: 10.1007/s40032-025-01163-2.
80. Chen X., Ma N., Liu H., Chen Y., Nie R., Zhang Z., Zhou J., Zhou Z. Study on immersion rotary helical electrode electrochemical discharge machining of Inconel 718 alloy. *Journal of Materials Research and Technology*, 2025, vol. 38, pp. 288–305. DOI: 10.1016/j.jmrt.2025.07.191.
81. Korgal A., Karanth P.N., Shettigar A.K., Madhavi J.B. A novel application of the micro-wire-electro-discharge-grinding (μ -WEDG) method for the generation of tantalum and brass nanoparticles. *Micro and Nano Systems Letters*, 2024, vol. 12 (1), pp. 1–19. DOI: 10.1186/s40486-024-00210-4.
82. Sharma A., Sharma N., Singh R.P., Arora R., Gill R.S., Singh G. Micro-drill on Al/SiC composite by EDD process: An RSM-MOGO based hybrid approach. *International Journal of Lightweight Materials and Manufacture*, 2022, vol. 5 (4), pp. 564–575. DOI: 10.1016/j.ijlmm.2022.07.002.
83. Korgal A., Shettigar A.K., Karanth N.P., Kumar N., Bindu M.J. Electro-discharge machining of microholes on 3d printed Hastelloy using the novel tool-feeding approach. *International Journal of Lightweight Materials and Manufacture*, 2025, vol. 8 (2), pp. 157–164. DOI: 10.1016/j.ijlmm.2024.10.005.

84. Goyal A. Investigation of material removal rate and surface roughness during wire electrical discharge machining (WEDM) of Inconel 625 super alloy by cryogenic treated tool electrode. *Journal of King Saud University – Science*, 2017, vol. 29 (4), pp. 528–535. DOI: 10.1016/j.jksus.2017.06.005.
85. Pandey A., Kumar R. Some studies using cryogenically treated rotary Cu-tool electrode electrical discharge machining. *Materials Today: Proceedings*, 2018, vol. 5 (2), pp. 7635–7639. DOI: 10.1016/j.matpr.2017.11.438.
86. Torres A., Puertas I., Luis C.J. Modelling of surface finish, electrode wear and material removal rate in electrical discharge machining of hard-to-machine alloys. *Precision Engineering*, 2015, vol. 40, pp. 33–45. DOI: 10.1016/j.precisioneng.2014.10.001.
87. Kumar S.V., Kumar M.P. Optimization of cryogenic cooled EDM process parameters using grey relational analysis. *Journal of Mechanical Science and Technology*, 2018, vol. 28, pp. 3777–3784. DOI: 10.1007/s12206-014-0840-9.
88. Tharian B.K., Dhanish P.B., Manu R. Enhancement of material removal rate in electric discharge machining of Inconel 718 using cryo-treated graphite electrodes. *Materials Today: Proceedings*, 2021, vol. 47, pp. 5172–5176. DOI: 10.1016/j.matpr.2021.05.506.
89. Datta R.S., Biswal B.B. Experimental studies on electro-discharge machining of Inconel 825 super alloy using cryogenically treated tool/workpiece. *Measurement*, 2019, vol. 145, pp. 611–630. DOI: 10.1016/j.measurement.2019.06.006.
90. Singh N., Routara B.C., Nayak R.K. Study of machining characteristics of Inconel 601 with cryogenic cooled electrode in EDM using RSM. *Materials Today: Proceedings*, 2018, vol. 5 (11), pp. 24277–24286. DOI: 10.1016/j.matpr.2018.10.223.

Conflicts of Interest

The authors declare no conflict of interest.

© 2025 The Authors. Published by Novosibirsk State Technical University. This is an open access article under the CC BY license (<http://creativecommons.org/licenses/by/4.0>).